Contents lists available at ScienceDirect

Journal of Controlled Release

journal homepage: www.elsevier.com

Non-invasive epicutaneous vaccine against Respiratory Syncytial Virus: Preclinical proof of concept

Pierre-Louis Hervé [a, *], Delphyne Descamps [b, 1], Charlotte Deloizy [b, 1, 2], Véronique Dhelft [a, 1], Daphné Laubreton [b], Edwige Bouguyon [b], Abdelhak Boukadiri [c], Catherine Dubuquoy [b], Thibaut Larcher [d], Pierre-Henri Benhamou [a], Jean-François Eléouët [b], Nicolas Bertho [b], Lucie Mondoulet [a, *, 3], Sabine Riffault [b, *, 3]

[a] DBV Technologies, 177-181 avenue Pierre Brossolette, 92120 Montrouge, France
[b] VIM, INRA, Université Paris-Saclay, 78350 Jouy-en-Josas, France
[c] GABI, INRA, Université Paris-Saclay, 78350 Jouy-en-Josas, France
[d] APEX, INRA, Rue de la Geraudière, 44000 Nantes, France

ARTICLE INFO

Article history:
Received 28 July 2016
Received in revised form 3 October 2016
Accepted 4 October 2016
Available online xxx

Keywords:
Respiratory Syncytial Virus
Cutaneous vaccine
Viaskin® patch
N-nanoring nanoparticle

ABSTRACT

To put a Respiratory Syncytial Virus (RSV) vaccine onto the market, new vaccination strategies combining scientific and technical innovations need to be explored. Such a vaccine would also need to be adapted to the vaccination of young children that are the principal victims of acute RSV infection. In the present project, we describe the development and the preclinical evaluation of an original epicutaneous RSV vaccine that combines two technologies: Viaskin® epicutaneous patches as a delivery platform and RSV N-nanorings (N) as a subunit antigen. Such a needle-free vaccine may have a better acceptability for the vaccination of sensible population such as infants since it does not require any skin preparation. Moreover, this self-applicative vaccine would overcome some issues associated to injectable vaccines such as the requirement of sterile medical devices, the need of skilled health-care professionals and the necessity of stringent store conditions. Here, we demonstrate that Viaskin® patches loaded with a formulation containing N-nanorings (Viaskin®-N) are highly immunogenic in mice and promotes a Th1/Th17 oriented immune response. More importantly, Viaskin®-N epicutaneous vaccine confers a high level of protection against viral replication upon RSV challenge in mice, without exacerbating clinical symptoms. In swine, which provides the best experimental model for the transcutaneous passage of drug/antigen in human skin, we have shown that GFP fluorescent N-nanorings, delivered epicutaneously with Viaskin® patches, are taken up by epidermal Langerhans cells. We have also demonstrated that Viaskin®-N induced a significant RSV N-specific T-cell response in pig. In conclusion, Viaskin®-N epicutaneous vaccine seems efficient to protect against RSV infection in animal model.

1. Introduction

The development of a safe and effective RSV vaccine for infants in the first six months of life is a public health challenge for reducing the severe burden of RSV-associated respiratory diseases, especially bronchiolitis and hospitalizations. Globally, it is estimated that RSV causes > 30 million lower respiratory tract infections each year resulting in > 3 million hospitalizations, making it the most common cause of hospitalizations in children under 5 [1]. Moreover, severe RSV incidence is highest in infants younger than 5 months.

Development of RSV vaccines has been complicated by the dramatic outcome of the first clinical trial in the 60′s, which examined the efficacy of a formalin-inactivated virus vaccine (FI-RSV) in infants and young children. Indeed, this vaccine formulation exacerbated clinical symptoms upon RSV infection and led to the hospitalization of almost 80% of the vaccinated children [2].

To date, there is no available vaccine against RSV. A large array of alternative vaccination strategies (antigen candidates and routes of administration) are being explored, but without providing satisfactory solutions [3–5]. There are indeed major challenges unique to RSV related to i) the young age of infection, ii) the failure of natural infection to induce immunity that prevents re-infection, and iii) the risk of immune-mediated disease exacerbation. Furthermore, due to the young age of the target population, a non-invasive and painless vaccine approach would be highly desirable.

In the present study, we evaluated a novel vaccination strategy against RSV that combines two original technologies: Viaskin® epicutaneous patches as a delivery platform (patent WO/2011/128430) [6] and RSV nucleoprotein nanorings (N-nanorings) as a subunit antigen (patents WO/2007/119011 and WO/2006/117456) [7,8]. Purified recombinant RSV N assembles as soluble nanorings of 15 nm diameter, composed of 10 to 11 N protomers bound to a bacterial RNA of

*Corresponding authors.
Email addresses: pierre-louis.herve@dbv-technologies.com (P-L Hervé); lucie.mondoulet@dbv-technologies.com (L. Mondoulet); sabine.riffault@jouy.inra.fr (S. Riffault)

[1] Contributed equally to the work.
[2] Present address: GenoSafe, 1 bis rue de l'International, 91000 Evry, France.
[3] L.M. and S.R. shared last co-authorship.

http://dx.doi.org/10.1016/j.jconrel.2016.10.003
0168-3659/

70 bases [9,10]. These N-nanorings, when administered intranasally, induce potent local and systemic immune responses in mice and calves and confer protection against an RSV challenge [11,12]. Protection afforded by N-nanorings in mice correlates with the presence of potent N-specific CD4 and CD8 T-cell responses [11]. N-nanorings are also able to induce a strong anti-N humoral response. However, these antibodies are non-neutralizing and passive transfer experiments performed in mice suggested that they possess no effective role in protection [11].

Skin has been recently explored as an original route for immunization, especially for the induction of a potent mucosal immune response against respiratory, gastro-intestinal or sexually transmissible pathogens [13]. Several vaccine strategies have been explored for the transcutaneous delivery of antigens [14]. However, due to the difficulty to get through the skin's top dead layer (*stratum corneum*), the vast majority of these approaches requires a preparation of the skin such as mechanical or chemical disruption, or the use of microneedles [15]. A few years ago, a novel epicutaneous delivery system was designed by DBV Technologies for food allergy desensitization [16]. This system is composed of patches (Viaskin® technology) that form an occlusive condensation chamber where allergen is solubilized by skin perspiration (skin hydration) and delivered across the stratum corneum to the epidermis without any skin preparation (see Graphical abstract) [16–22]. More recently, DBV Technologies got the proof-of-concept that Viaskin® patches can also be used as an efficient vaccine delivery platform in a murine model, in the context of *Bordetella pertussis* (*B. pertussis*) booster vaccine development [23]. Indeed, a single application of Viaskin® patch loaded with genetically-detoxified pertussis toxin (rPT), in the absence of adjuvant, was able to efficiently recall memory vaccine-induced immunity against *B. pertussis*.

The skin barrier is composed of a dense network of antigen presenting cells (APCs), including dendritic cells (DC) such as Langerhans cells (LC) that resides in the epidermis layer [24]. These DC provide immune-surveillance by "sensing" pathogens passing through stratum corneum and play a central role to activate the adaptive immunity. Our group has pioneered the characterization of DC subsets within the skin of pig and shown that it shares many similarities with human skin DC [25]. In fact, pig skin histology is very similar to the human one's and is thus recognized as one of the most appropriate model to study delivery of pharmaceutical compounds *via* skin [25–27]. Thus we investigated in piglets whether fluorescent N-nanorings fused to GFP would reach skin immune cells when administered with the Viaskin® platform. We observed both an internalization of N-GFP antigen by skin Langerhans cells and the induction of antigen-specific cellular immune responses in spleen.

The immunization procedure with N-nanorings-loaded Viaskin® patches (Viaskin®-N) was further investigated in mice in order to characterize the antiviral immune response elicited and its capacity to protect against challenge with an RSV-Luciferase recombinant virus. Viaskin®-N vaccination elicited a strong antigen-specific cellular response in mice and piglets. In mice, Viaskin®-N promotes a Th17/Th1 oriented immune response and conferred protection against virus replication in lungs.

2. Material and methods

2.1. Plasmid construction, protein expression and purification of N-nanorings

Expression and purification of recombinant nucleoprotein (N) was performed as previously described [9]. Briefly, the purification of the recombinant N protein is permitted by its specific interaction with the C-terminal region of RSV P protein (PCT) (residues 161–241) fused to GST. *E. coli* BL21 (DE3) bacteria were co-transformed with pGEX-PCT and pET-N and then grown at 37 °C for 8 h in 1 L of Luria-Bertani (LB) medium containing 100 μg/mL of ampicillin and 50 μg/mL of kanamycin. The same volume of LB medium was then added, and protein expression was induced by adding 80 μg/mL isopropyl-β-D-thiogalactopyranoside (IPTG) to the medium. Bacteria were incubated for a further 15 h at 28 °C and harvested by centrifugation. Protein complexes were purified from the bacterial pellets on glutathione-sepharose 4B beads (GE Healthcare, Uppsala, Sweden) as previously described [28]. To isolate N-nanorings, beads containing bound complexes were incubated with biotinylated thrombin (Merck Millipore, Darmstadt, Germany) for 16 h at 20 °C. Thrombin was then removed using the cleavage capture kit according to the manufacturer's instructions (Merck Millipore, Darmstadt, Germany). Purified N-nanorings were then concentrated on Vivaspin® centrifugal concentrator (Sartorius, Goettingen, Germany) and sterilely filtered. Of note, a small amount of PCT was co-purified with chimeric N-nanorings. However, we previously demonstrated that PCT is poorly immunogenic and induced a low anti-P antibody response by comparison with the entire P protein [29]. N-nanorings fused to Green Fluorescent Protein (N-GFP) was constructed as previously described [11]. Briefly, the EGFP coding sequence was cloned onto pET-N plasmid. The resulting plasmid was designated as pET-N-GFP and encode for a chimeric N protein fused to EGFP at its C-terminus. The expression and the purification protocols of N-GFP were identical to those of N protein alone.

2.2. Production of N-nanorings-loaded Viaskin® patches (Viaskin®-N)

N- and N-GFP- nanorings were purified as described above. Then, a homogeneous mix between N- or N-GFP nanorings and CpG was made in PBS to a respective concentration of 1 mg/mL. 50 μL (mice immunization) or 100 μL (piglets immunization) were then homogeneously deposited on Viaskin® patches and dried 1 h at 30 °C in a ventilated oven to produce Viaskin®-N and Viaskin®-N-GFP, respectively. The stability of N-nanorings after their deposition on Viaskin® patches was then controlled by native gel electrophoresis, electronic microscopy and DLS after recovery from the matrix of the patch (Fig. S1). Results showed that N-nanorings integrity was preserved upon deposition and drying on Viaskin® patches.

2.3. Mice: immunization, challenge protocols and sample collection

Female BALB/c mice aged 6 weeks were purchased from Janvier's breeding center (Le Genest, St Isle, France) and housed under Bio-Safety Level (BSL)-2 conditions in the animal facility (IERP, INRA, Jouy-en-Josas, France). All experiments were carried out in INRA (Rodent Experimental Infectiology Platform, Jouy-en-Josas, France) and approved by the ethics committee COMETHEA (ETHical COMmittee for Animal Experimentation, INRA and AgroParisTech; authorization number 12-126). All efforts were made to optimize animal welfare (environmental enrichment) and avoid suffering.

For Viaskin® patches immunization, mice were anesthetized with a solution of ketamine and xylazine (50 and 10 mg/kg respectively) and hairs were removed from the back of each mouse using an electric clipper and then a depilatory cream (Veet®, Reckitt Benckiser, Slough, Berkshire, United Kingdoms). N-rings loaded Viaskin® (Viaskin®-N) was applied on the depilated back the day after and secure using a bandage (Urgoderm® band-aid, Urgo laboratories, Chenôve, France).

For intra-nasal immunizations, mice were anesthetized with a solution of ketamine and xylazine (50 and 10 mg/kg respectively) and

vaccinated twice at 2 weeks interval by intra-nasal instillation of 50 μL of 0.9% endotoxin-free NaCl, containing 10 μg of N-nanorings, associated to 10 μg of CpG ODN (1826) (T*C*C*A*T*G*A*C*G*T*T*C*C*T*G*A*C*G*T*T, Sigma-Aldrich, Saint Louis, Missouri).

For intra-dermal immunizations, mice were anesthetized with a solution of ketamine and xylazine (50 and 10 mg/kg respectively) and vaccinated twice at 2 weeks interval by intra-dermal injection of 50 μL of 0.9% endotoxin-free NaCl, containing 10 μg of N-nanorings, associated to 10 μg of CpG ODN (1826).

Two weeks after the last Viaskin® or intra-nasal immunization, mice were anesthetized and inoculated intra-nasally with 8.8×10^4 PFU of RSV-Luciferase virus [30]. This recombinant virus was generated from RSV Long strain and expresses firefly luciferase in infected cells, allowing us to detect viral replication in living mice *via* the luminescence emitted after the transformation of D-luciferin substrate into oxyluciferin. Of note, this virus presents the same virulence as RSV Long WT and luminescence values measured from infected animals fully correlate with viral replication as previously described [30]. After infection, body weight and clinical score were monitored daily.

Blood samples were collected *via* cheek puncture at day 0 (before immunization), day 14 and 35. At autopsy, mice were killed by cervical dislocation. Broncho-alveolar lavages (BAL) were performed by flushing the lungs *via* tracheal puncture two times in and out with 1 mL of Ca^{2+}- and Mg^{2+}-free PBS supplemented with 1 mM EDTA. BAL fluids were centrifuged 5 min at $250 \times g$ and supernatants were stored frozen at − 20 °C for anti-N antibody titers measurement.

2.4. Piglets: Viaskin® immunization protocol and sample collection

Piglets were purchased and housed in our animal facility (INRA, IERP, Nouzilly, France). All experiments were carried out in INRA (Experimental Infectiology Platform, Nouzilly, France) and approved by the ethics committee CEEA VdL (Ethical Committee for Animal Experimentation, Val de Loire; authorization number CEEA VdL N°19). All efforts were made to optimize animal welfare (environmental enrichment) and avoid suffering.

For the study of the passage of N-GFP through the skin, 4 weeks old piglets were shaved and depilated on their flanks using an electric depilator. N-GFP loaded Viaskin® (Viaskin®-N-GFP) was applied on the depilated flank the day after and secure using Tegaderm® bandage (3M, Saint Paul, Minnesota) and Elastoplast® band-aid (Beiersdorf, Hamburg, Germany). Viaskin®-N-GFP was applied for 24 h or 48 h and piglets were autopsied 24 h after Viaskin® removal or just after Viaskin® removal. At autopsy, piglets were slightly anesthetized, then euthanized with an intra-cardiac injection of Dolethal® (Vetoquinol, Magny-Vernois, France). Skin samples were then collected from the area corresponding to patches location. Skin sample was immediately frozen in Tissue-Tek® O.C.T. embedding solution (Sakura Finetek, Tokyo, Japan) for subsequent histological analysis.

For immunogenicity study, 8 weeks old piglets were shaved and depilated on their flanks using an electric depilator. After 24 h, Viaskin® patches loaded with N-nanorings and swine CpG ODN (G*GTGCATCGATTTATCGATTATCGATGCAGG*G*G*G*G, Sigma-Aldrich, Saint Louis, Missouri) was applied on their left flank and secured as described above. Viaskin®-N application was repeated 6 times during 3 contiguous weeks, modelling the immunization protocol that have been implemented in mice. Alternatively, piglets were immunized by intra-muscular injection, twice at two weeks interval, with 20 μg of N-nanorings, adjuvanted with Montanide™ ISA 71 VG. Blood and nasal swab samples were collected before and every week after the first immunization, during 5 weeks. Piglets were autopsied 2 weeks after the last Viaskin®-N application. Piglets were euthanized as described above and spleen were collected for *in vitro* stimulation of T-cells.

2.5. Evaluation of anti-N antibody responses by ELISA

Individual mouse sera and BAL were assayed for anti-N antibodies (Ig(H + L), IgG2a, IgG1 or IgA) by indirect ELISA using N nanorings as the capture antigen (200 ng per well on microplates), as previously described [11]. Individual piglet sera were assayed similarly for anti-N antibodies using HRP-conjugated anti swine Ig(H + L) secondary antibody (Jackson ImmunoResearch, West Grove, Pennsylvania). End-point antibody titers were calculated by regression analysis, plotting serum dilution *versus* the absorbance at 450 nm using Microcal Origin (OriginLab Corporation, Northampton, Massachusetts) (regression curve $y = ((b + cx) / (1 + ax))$. Endpoint titers were defined as the highest dilution resulting in an absorbance value twice that of blank points (points realized with diluent buffer).

2.6. Evaluation of N-specific T-cell response in mice and piglets

For mice experiment, spleen were collected two weeks after the last immunization and gently homogenized in RPMI medium using a 100 μm nylon cell-strainer (Falcon). Red blood cells were depleted using 150 mM NH_4Cl and splenocytes were adjusted to 2.10^6 viable cells/mL in RPMI supplemented with 10% of foetal calf serum (FCS) and 2 mM L-glutamine. Then, 4.10^5 cells/well were distributed in 96-well flat-bottomed microtiter plates. Cells were then incubated in triplicates with either N-nanorings (10 μg/mL final concentration in RPMI medium) or RPMI medium alone as a negative control. Cell cultures were incubated at 37 °C in 5% CO_2, and supernatants were harvested 72 h later. Supernatants were assayed for IFN-γ and IL-5 by standardized ELISA (BD biosciences, Franklin Lakes, New Jersey) as previously described [31] or by multiplex analysis as described below.

For piglet experiment, spleen were collected two weeks after the last immunization and gently homogenized in PBS-Citrate 1.3 mM medium using a 100 μm nylon cell-strainer (Falcon). Red blood cells and cell debris were then eliminated by ficoll density gradient centrifugation, 30 min at $1000 \times g$. Spleen cells were stained with 2 μM CarboxyFluorescein Succinimidyl Ester (CFSE, ThermoFisher, Waltham, Massachusetts) 10 min at room temperature (RT). Then, 6.10^5 cells per well were deposited on microplates and mix with N-nanorings (10 μg/mL final concentration in Xvivo medium) or Xvivo medium alone as a negative control. Cell cultures were incubated at 37 °C in 5% CO_2 for 72 h and supernatants were harvested for measuring IFN-γ by ELISA. Fresh Xvivo medium was then added on each well and cells were incubated for another 48 h. Finally, cells were collected for immuno-staining and FACS analysis.

2.7. Measure of swine IFN-γ secretion by sandwich ELISA

Spleen cells collected from immunized piglets were stimulated *in vitro* as described above. Cell culture supernatants were collected at 72 h post-stimulation and were assayed for IFN-γ concentration by sandwich ELISA. To that end, microplates were coated with 200 ng of mAb-pIFN-γ (Mabtech, Cincinnati, Ohio) overnight at 4 °C. Plates were saturated with PBS 1 × tween 20 0.05% + 0.1% bovine serum albumin (BSA) 1 h at RT and 100 μL of cell culture supernatants were added for 2 h at RT. Bounded IFN-γ was detected by subsequent

incubations with mAb PAN-biotin (Mabtech, Cincinnati, Ohio) (0.5 mg/mL final concentration) for 1 h at RT and HRP-conjugated streptavidin (1 μg/mL final concentration) for 1 h at RT. HRP enzymatic activity was finally revealed using a 1-step Ultra TMB substrate (Thermo Scientific, Waltham, Massachusetts) and optical density was read at 450 nm wavelength using an Infinite® 200 pro Microplates reader (Tecan, Männedorf, Switzerland).

2.8. Antibodies and FACS staining

For skin passage study in piglets, skin cells were labelled and analyzed as previously described [25]. Briefly, skin samples were incubated overnight at 37 °C in RMPI complemented with 10% FCS containing 0.5 mg/mL of DNase I and 1 mg/mL of collagenase, and filtered on 100 μm nylon cell-strainer (Falcon). Cells were then collected and enriched in low-density cells such as dendritic cells and macrophages by OptiPrep density gradient (Sigma-Aldrich, Saint Louis, Missouri) as previously described [32]. Cells were then blocked in PBS containing 5% of horse serum for 20 min and incubated with anti-CD1 76-7-4, anti-SIRPα 74-22-15, anti-MHC-II Th21A (from Monoclonal Antibody Center, Washington State University, Pullmann, WA), anti-CD163 3A10 (ABD Serotec, Oxford, United-Kingdoms), anti-CD11c (in house clone 3A8) antibodies containing 5% horse serum for 1 h. These markers permit to discriminate between the different skin DC sub-populations. Cells were washed in PBS complemented with 2 mM EDTA and finally incubated with relevant fluorophore-conjugated isotype-specific secondary antibodies (Thermo Scientific, Waltham, Massachusetts). GFP signal was measured from these different sub-populations by FACS analysis. Cells were acquired and analyzed using an LSRFortessa cytometer and the Diva software (Becton Dickinson, Franklin Lakes, New Jersey) and results were analyzed using the FloJow software (FloJow, LLC, Ashland, Oregon).

For piglet immunization study, spleen cells collected from immunized piglets were stained with CFSE and stimulated *in vitro* as described above. Stimulated cells were collected at 5 days post-stimulation. Cells were then stained with 7-Aminoactinomycine D (7-AAD) to exclude dead cells and with anti-CD3 (8E6), anti-CD4 (74-12-14) and anti-CD8 (76-2-11) antibodies associated to relevant fluorophore-conjugated secondary antibodies following the protocol described above. Cells were acquired and analyzed as mentioned above. The gating strategy is described in Supplementary Figure 2 (Fig. S2).

For mice immunization study, spleen cells collected from immunized mice were stained with CFSE and stimulated *in vitro* as described above. Stimulated cells were collected at 5 days post-stimulation. Cells were then stained with anti-CD3, anti-CD4 and anti-CD8 antibodies conjugated to relevant fluorophores (Sony Biotechnology, Tokyo, Japan) in PBS containing 2% SVF. Cells were additionally stained with Zombie Aqua to exclude dead cells. Cells were then fixed and permeabilized using the Foxp3/Transcription Factor Fixation/Permeabilization buffer (eBioscience, San Diego, California) and stained with anti-FoxP3, anti-T-bet, anti-GATA-3 and anti-RORγt conjugated to relevant fluorophores (Sony Biotechnology, Tokyo, Japan). Cells were acquired and analyzed as mentioned above. The gating strategy is described in Supplementary Figure 3 (Fig. S3).

2.9. Immuno-histological staining of skin samples

Piglet skin were snap frozen in OCT (Sakura, Paris, France) and cryosections were mounted on glass slides (Superfrost plus, Thermo Scientific). Cryosections were air-dried and fixed and permeabilized using cold acetone/methanol bath and then blocked in PBS containing 5% of horse serum and 5% of swine serum. Slides were incubated with rabbit anti-N Ig, mouse anti-MHC-II IgG2a and mouse anti-CD163 IgG1 primary antibodies. Slices were then extensively washed in PBS and incubated with AF488 anti-rabbit IgG, AF55 anti-mouse IgG2a and AF647 anti-mouse IgG1 secondary antibodies. Finally, slices were stained with DAPI. Slides were observed using a fluorescent microscope coupled to a high resolution Pannoramic digital slide scanner and images were analyzed using Case Viewer software (3DHISTECH, Budapest, Hungary).

2.10. Production of recombinant RSV-luciferase fused for viral challenge

For viral challenges, we used a recombinant RSV containing the firefly luciferase gene (RSV-luciferase). This recombinant virus allows the visualization of infected cells in living mice, *via* the emission of luminescence [30]. For the production of viral stocks used for challenge, RSV-luciferase was amplified on HEp-2 cells at a low multiplicity of infection (10^{-3}) to eliminate potential defective interfering particles. Infected cells were gently shaken each day to detach syncytia and spread the infection to the whole cell monolayer. After 3 days, supernatant and infected cells were both collected using a Cell Scraper. Cell suspension was then sonicated 2 × 1 min to dissociate viral particles from cells and clarified by centrifugation 5 min at 400 × *g*. Supernatant was aliquoted and flash-frozen using a mix of ethanol absolute and dry ice. Aliquots were then immediately stored at − 80 °C.

2.11. Determination of RSV viral load in living mice

Viral loads were measured in living mice *via* photon emission that was representative of RSV-Luciferase replication, as previously described [30]. Briefly, mice were anesthetized with a solution of ketamine and xylazine (50 and 10 mg/kg respectively) and 0.75 mg/kg of D-luciferine (Sigma-Aldrich, Saint Louis, Missouri) diluted in sterile PBS was instilled intranasally. Viral replication was estimated 5 min later using an *In Vivo* Imaging System (IVIS-200) and Live Imaging software (Xenogen Advanced Molecular Vision, Grantham, United Kingdom's), by measuring the photon emission from Regions of Interest (ROI). Alternatively, lungs were homogenized in 500 μL of Passive Lysis Buffer (PLB) (1 mM Tris pH 7.9; 1 mM MgCl2; 1% Triton × 100; 2% glycerol; 1 mM DTT) with a Precellys 24 bead grinder homogenizer (Bertin Technologies, St Quentin en Yvelines, France) 2 × 15 s at 4 m/s. Lung homogenates were clarified by centrifugation 5 min at 2000 × *g* and distributed on microplates. Then, 1 μg/mL (final concentration) of firefly luciferine in PLB complemented with 0.5 mM of ATP was added on each well and photon emission was measured using the IVIS system (Xenogen, Advanced Molecular Vision). ROIs were defined in order to fit to lungs in living mice or to each wells in microplates. Photon emission measured from ROIs was expressed in photons per *sec*ond. The colorimetric scale used in mice photograph is expressed in radiance (photons/sec/cm^2/sr), which is the number of photons (p) per second (sec) that leave a square centimeter (cm^2) of tissue and radiate into a solid angle of one steradian (sr).

2.12. May-Grünwald-Giemsa staining and histology in mice

BAL cells isolated from individual mice were numerated, spread on microscope Superfrost™ slides (Thermo Scientific, Waltham, Massachusetts) by cytocentrifugation (5 min at 700 × rpm) using Shandon Cytospin® 5 (Thermo Scientific, Waltham, Massachusetts) and stained with May-Grünwald and Giemsa. At least 400 leukocytes were counted blindly for each sample.

Lungs collected at day 11 post-infection were fixed with PBS containing 10% paraformaldehyde (PBS-PFA), embedded in paraffin and 5 mm sections and finally mounted on glass slides (Superfrost plus, Thermo Scientific). Slides were stained by Hematoxylin Eosin Safran (HEC) or alcian blue. Slides were observed using a bright-field microscope coupled to a high resolution Pannoramic digital slide scanner and images were analyzed using Case Viewer software (3DHISTECH, Budapest, Hungary). Images were analyzed and interpreted by an independent professional histopathologist.

2.13. Measure of cytokine concentration by multiplex analysis

Cytokine levels were measured from mouse BAL or lung homogenates using a mouse cytokine & chemokine panel 1 Affymetrix ProcartaPlex® Multiplex immunoassay (eBioscience, San Diego, California), following manufacturer instructions. Cytokine levels were measured from spleen culture supernatants using a Bio-Plex Pro™ Mouse Cytokine Immunoassay (Bio-Rad, Hercules, California), following manufacturer instructions. Data were acquired using a Bio-Plex® multiplex system (Bio-Rad, Hercules, California). Results were analyzed using ProcartaPlexAnalyst software (eBioscience, San Diego, California) or using the Bio-Plex® software (Bio-Rad, Hercules, California).

2.14. Statistical data analysis

Data were expressed as arithmetic mean ± Standard Error of the Mean (SEM). Non-parametric Mann-Whitney test was used to compare unpaired values (GraphPad Prism® software, San Diego, California). Values of $P < 0.05$ were considered significant. The level of significance is indicated on the graphs with asterisks: * $P < 0.05$; ** $P < 0.01$; *** $P < 0.001$ and **** $P < 0.0001$.

3. Results

3.1. N-rings administered via Viaskin® patches target Langerhans cells (LC) in piglet skin

We first evaluated the capacity of N antigen to reach and target cutaneous dendritic cells (DC) when administered with Viaskin® patches in piglets. For that purpose, we used N-nanorings fused to GFP (N-GFP) whose fluorescence can be tracked *in vivo* and *ex vivo* (Fig. 1). Piglets received Viaskin®-N-GFP for 48 h and were sacrificed 24 h after patch removal (group 1) or received Viaskin®-N-GFP for 24 h and were sacrificed just after patch removal (group 2). For each piglet, a skin biopsy corresponding to Viaskin®-N-GFP application area was collected from both flanks (Fig. 1A). Fluorescence microscopy results, obtained from skin cryosections, showed a close co-localization between the GFP signal and the *stratum corneum* for group 2 (left flank). Conversely, no GFP signal was detected at the skin surface for group 1, suggesting that N-GFP protein was washed away from the *stratum corneum* over the 24 h interval between patch removal and autopsy (Fig. 1B). Few rare GFP signals could be detected in skin sections of the group 2 (Fig. 1C), co-localizing with MHC-II^{high} cells. We then chose flow cytometry, a much more sensitive method for faint and rare events, and used a previously described gating strategy allowing us to discriminate the different DC and macrophages populations of the swine skin [25]. We were able to detect a significant increase of GFP signal in Langerhans cells (LC) of the group 1 ($P < 0.05$), but not in other DC subtypes (cDC-1 and cDC-2) (Fig. 1D). Overall, these data indicate that N-nanorings delivered epicutaneously by Viaskin® patches are efficiently captured by epidermal LC. This encouraging result prompted us to analyze the nature of the immune response that could be induced by Viaskin®-N immunization in mice and piglet, as well as the protection afforded in an experimental mouse model of RSV infection.

3.2. Implementation of an epicutaneous vaccination protocol with Viaskin®-N in mice

The Viaskin®-N formulation and immunization schedule were optimized in BALB/c mice. We used CpG ODN as an adjuvant to promote Th1 responses known to be important for safe and protective RSV vaccination, especially in the context of neonates [33].

Mice immunized with Viaskin®-N and CpG ODN developed significant titers of anti-N antibodies after three patch applications, both of IgG1 and IgG2a isotypes (mean antibody titers of 2.9 ± 1.5 log10 *versus* < 1.5 log10 for the control group, $P < 0.05$; 2.7 ± 1.4 log10 *versus* < 1.5 log10 for the control group, $P < 0.05$, respectively) (Fig. 2B). Conversely, our previous data showed that mice immunized with Viaskin®-N without CpG ODN exclusively developed anti-N IgG1 antibody titers after three applications (data not shown). Then, to monitor mucosal immunity, anti-N IgG1, IgG2a and IgA antibody responses were evaluated in broncho-alveolar lavages (BAL) collected at autopsy (Fig. 2C). Anti-N IgG1 and IgG2a were detectable only in immunized mice (mean antibody titers of 1.2 ± 0.8 log10 *versus* < 0.5 log10 for the control group, $P < 0.05$ and 1.0 ± 0.9 log10 *versus* < 0.5 log10 for the negative control group, $P = 0.08$, respectively). However, no specific IgA were detected (mean antibody titers < 0.5 log10). Finally, N-specific cellular response was evaluated in Viaskin®-N immunized mice from spleen cells collected at autopsy and stimulated *in vitro* with N-nanorings (Fig. 2D). Spleen cells collected from the Viaskin®-N immunized mice secreted IFN-ϒ ($P < 0.05$ compared to the control group) and, to a lower amount, IL-5 (non-significant compared to the control group).

In an attempt to augment the magnitude of these immune responses and reduce their variability, we increased the number of patch application up to 6 of 48 h each (Fig. 3A). We also compared our Viaskin®-N epicutaneous immunization to intra-nasal and intra-dermal routes. Mice immunized with Viaskin®-N and CpG-ODN developed higher levels of anti-N antibodies in sera than in the previous experiment described in Fig. 2 (mean IgG1 titer of 6.1 ± 0.3 log10 *versus* 1.5 ± 0.1 for the control group at day 35, $P < 0.001$; mean IgG2a titer of 5.6 ± 0.8 log10 *versus* 1.6 ± 0.3 for the control group at day 35, $P < 0.001$) (Fig. 3B). These titers were slightly but significantly lower than those induced by intra-nasal immunization (mean IgG1 titer of 6.8 ± 0.3 log10; mean IgG2a titer of 7.1 ± 0.2 log10 at day 35) or intra-dermal immunization (mean IgG1 titer of 6.6 ± 0.2 log10; mean IgG2a titer of 6.9 ± 0.2 log10 at day 35). Interestingly, similar levels of IgG1 and IgG2a isotypes were obtained for all routes of immunization with, however, a slightly higher IgG1/IgG2a ratio for Viaskin®-N immunized mice (mean ratio of 12.3 ± 17.8 *versus* 0.8 ± 1.1 for intra-nasal, $P = 0.09$ *versus* 0.2 ± 0.2 for intra-dermal, $P = 0.05$). In BAL, mice immunized with Viaskin®-N developed significant levels of anti-N Ig(H + L) (mean antibody titer of 3.6 ± 0.3 log10 *versus* 0.9 ± 0.3 log10 for the control group, $P < 0.001$) that was slightly lower than those induced by intra-nasal or intra-dermal immunizations (mean antibody titers of 4.7 ± 0.2 log10 for intra-nasal and 4.0 ± 0.1 log10 for intra-dermal), whereas IgA were exclusively induced by intra-nasal immunization (mean antibody titers of 2.1 ± 0.1 log10, $P < 0.001$) (Fig. 3C). Of note, anti-N antibody titers were still dispersed upon Viaskin®-N vaccination compared to intra-nasal or intra-dermal immunizations. However, this dispersion

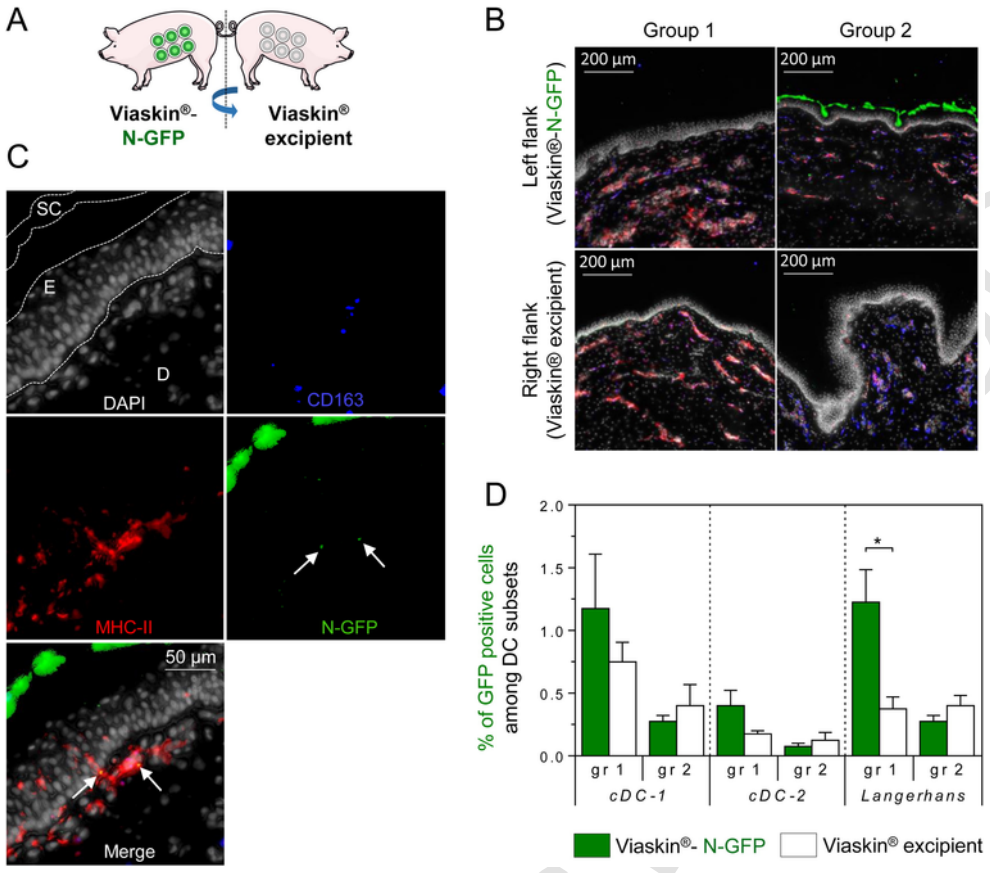

Fig. 1. N-nanorings delivered *via* Viaskin® patches are captured by Langerhans cells in piglet skin. (A) 2 groups of piglets received 6 Viaskin® patches loaded with 100 µg of N-nanorings fused to Green Fluorescent Protein (GFP) and 100 µg of CpG on their left flank (Viaskin®-N-GFP). As a negative control, the same piglets received 6 Viaskin® patches loaded with 100 µg of CpG alone on their right flank (Viaskin® excipient). This skin area has been selected from perspiration measurement data, showing that the flank generated a sufficient level of humidity (perspiration). Perspiration values were also indicative of a good skin integrity (data not shown). Group 1 received Viaskin®-N-GFP for 48 h and was autopsied 24 h after Viaskin® removal. Group 2 received Viaskin®-N-GFP for 24 h and was autopsied just after Viaskin® removal. At autopsy, skin samples were collected and frozen in embedding solution. Skin frozen sections were prepared, then fixed, permeabilized and incubated with rabbit anti-N Ig, mouse anti-MHC-II IgG2a and mouse anti-CD163 IgG1 primary antibodies associated to relevant fluorophore-conjugated secondary antibodies. (B) A representative photograph of one section of each group is shown. (C) Photograph of a skin section collected from a piglet of the group 2, showing GFP signal in Langerhans cells (SC: *stratum corneum*, E: epidermis, D: dermis). (D) Cells were isolated from skin samples of the groups 1 and 2, by overnight dispase/collagenase digestion. Skin cells were then incubated with anti-CD163, anti-CD172 (SIRP) and anti-MHC-II (MSA3) antibodies associated with relevant fluorophore-conjugated secondary antibodies. Cells were analyzed using an LSR Fortessa flow cytometer. Gating of cDC-1, cDC-2 and Langerhans cells was done as previously described [25]. Data are mean + SEM of individual values (n = 4 per experimental group), expressed as the individual % of GFP positive cells among each of the skin DC subpopulations. *P* values were determined according to the Mann-Whitney test (*, $P < 0.05$). (For interpretation of the references to color in this figure legend, the reader is referred to the web version of this article.)

was largely reduced compared to the results obtained in the previous set of experiment described in Fig. 2 (standard deviations of 1.6 log10 for IgG1 and 1.4 log10 for IgG2a after 3 patches applications in Fig. 2 *versus* 0.3 log10 for IgG1 and 0.8 log10 for IgG2a after 6 patches applications in Fig. 3).

Having defined an optimized Viaskin®-N immunization protocol in mice, we then undertook to better qualify, in mice and piglets, the type of cellular memory responses that have been primed.

3.3. Viaskin®-N epicutaneous immunization induces strong CD4 and CD8 antigen-specific memory responses in mice and piglets

N-specific cellular response was evaluated from spleen leukocytes that were collected at autopsy from immunized mice (Fig. 4) or piglets (Fig. 5) and further stimulated *in vitro* with N-nanorings.

In mice, a similar and significant increase of CD4 and CD8 T-cell percentages was noticed for Viaskin®-N, intra-nasal or intra-dermal groups compared to the control group (Fig. 4A). Importantly, the Viaskin®-N group was the only vaccinated group showing a significant increase of CD4 and CD8 T-cell antigen-specific proliferation. In CD4 T-cells, the percentages of T-Regs, Th1, Th2 and Th17 subpopulations were significantly increased for Viaskin®-N and intra-nasal groups (Fig. 4B). For T-Regs and Th17, this increase was accordingly associated with a significant secretion of IL-10 and IL-17. Additionally, T-Reg and Th17 antigen-specific proliferation was significantly higher for the Viaskin®-N group compared to the control group. The Viaskin®-N group presented a higher percentage of Th2 cells ($P < 0.05$ *versus* intra-nasal and $P < 0.01$ *versus* intra-dermal) that was accordingly associated with an increase of Th2 cytokines concentration ($P < 0.05$ *versus* intra-nasal; $P < 0.001$ *versus* intra-dermal for IL-13; $P < 0.01$ *versus* intra-nasal and $P < 0.001$ *versus* intra-dermal for IL-5) and the level of IFN-γ was significantly lower ($P < 0.01$ *versus* intra-nasal or intra-dermal) (Fig. 4B). Of note, the level of IFN-γ was higher than the level of Th2 cytokines for both vaccinated groups (mean IFN-γ/IL-5 ratio of 14 ± 9 for Viaskin®-N, 148 ± 122 for intra-nasal and 882 ± 601 for intra-dermal; mean IFN-γ/IL-13 ratio of 3.3 ± 2.2 for Viaskin®-N, 23.4 ± 19.6 for intra-nasal and 90.3 ± 35.6 for intra-dermal), suggesting that the Th1 response was generally predominant regardless of the route of immunization. Interestingly, the levels of IL-2 (involved in the differentiation and the

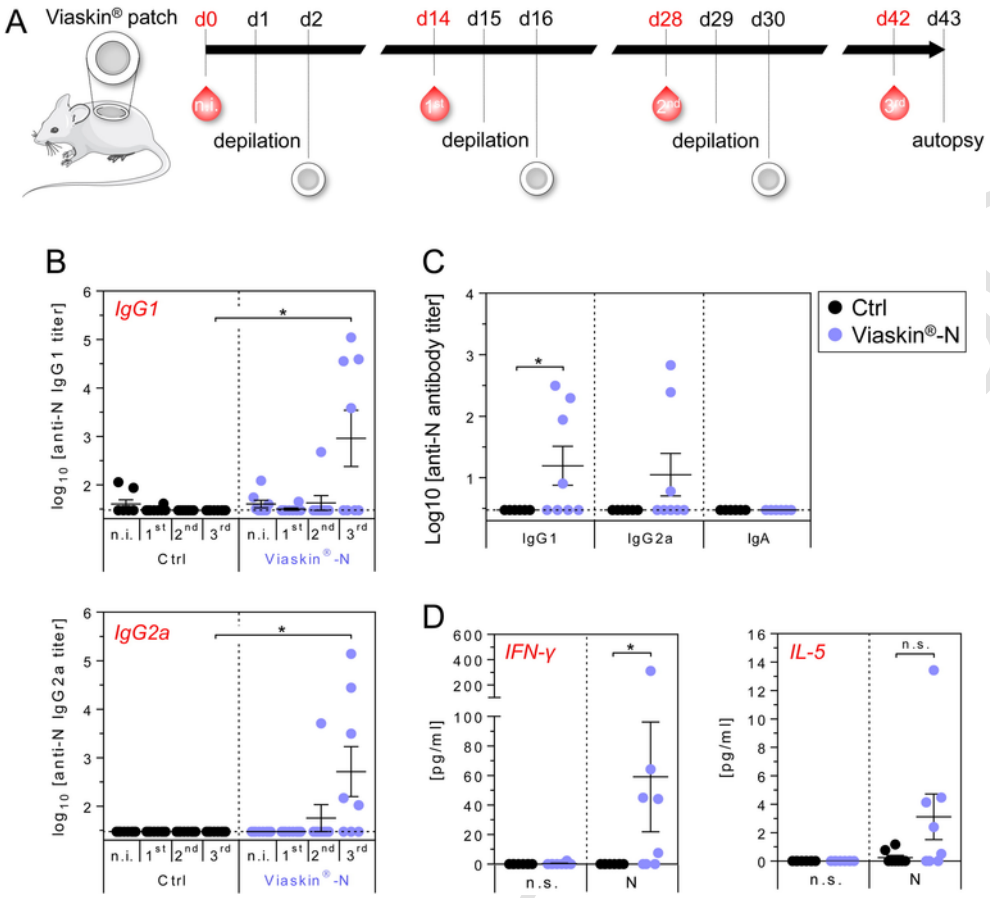

Fig. 2. Antibody and cellular responses induced by Viaskin®-N epicutaneous immunization. (A) BALB/c mice were epicutaneously immunized with Viaskin® patches loaded with 50 μg of N-nanorings and 50 μg of CpG ODN as adjuvant (Viaskin®-N). Viaskin®-N patches were applied for 48 h on depilated back, three times at two weeks interval, as indicated. 48 h has been defined as the best application timing for the induction of an optimal specific immune response in a previous set of experiment (data not shown). As a negative control, mice received 3 patches loaded with excipient alone (PBS) and 50 μg of CpG (Ctrl, in black). (B) N specific IgG1 (upper panel) and IgG2a (lower panel) titers were evaluated by indirect ELISA using N-nanorings as a coating, in sera prepared from blood samples collected before (non-immunized: n.i.) or two weeks after the first (1st), the second (2nd) or the third (3rd) Viaskin® application (schematized by a red blood drop in panel A). (C) N specific IgG1, IgG2a and IgA were measured by indirect ELISA using N-rings as a coating, in BAL fluids collected at autopsy. (D) Splenocytes were then stimulated *in vitro* with RPMI medium (negative control, non-stimulated: n.s.) or N-nanorings (N). IFN-ϒ (left-panel) and IL-5 (right panel) concentrations were measured from cell culture supernatants collected 72 h post-stimulation. Data are mean ± SEM of individual antibody titers for each group (n = 7–8 per experimental group). *P* values were determined according to the Mann-Whitney test (*, $P < 0.05$; n.s., non-significant). (For interpretation of the references to color in this figure legend, the reader is referred to the web version of this article.)

proliferation of T-cells but also in the maintenance of Tregs [34]) and GM-CSF (involved in the regulation of T-cell function) were higher in the Viaskin®-N group ($P = 0.05$ *versus* intra-nasal and $P < 0.001$ *versus* intra-dermal for IL-2; $P < 0.05$ *versus* intra-nasal and $P < 0.01$ *versus* intra-dermal for GM-CSF) (Fig. 4C).

In piglets, a strong secretion of IFN-γ was observed in leukocyte culture supernatant at 48 h for the intra-muscularly vaccinated group ($P < 0.001$ compared to the negative control group) (Fig. 5B). IFN-γ secretion was also observed for Viaskin®-N vaccinated piglets albeit at a lower level ($P = 0.1$ compared to the negative control group). However, Viaskin®-N immunized piglets had an increased proliferation of CD4 and CD8 T-cells as well as of CD4/CD8 negative T-cells (*bona fide* γδ T-cells) compared to the negative control group ($P = 0.05$ for CD4 T-cells, $P = 0.09$ for CD8 T-cells and $P = 0.03$ for γδ T-cells) (Fig. 5C). This level of proliferation was similar to that measured for splenocytes obtained from intra-muscular immunized group. Interestingly, no antibody induction was observed in Viaskin®-N immunized piglets.

To conclude, N-nanorings associated to CpG ODN and administered repeatedly using Viaskin® patches are highly immunogenic in mice and piglets and are particularly efficient at inducing both CD8 and CD4 T-cell responses. Interestingly, the T-cell response primed by Viaskin®-N epicutaneous vaccine in mice was quite different than the one induced by intra-dermal immunization in terms of magnitude and orientation, especially concerning T-CD8 and Th17 responses, despite the vicinity of these two vaccination routes.

3.4. Viaskin®-N epicutaneous immunization protects mice against RSV infection

After challenging vaccinated mice with an RSV-luciferase recombinant virus, viral replication was monitored in lungs at day 4 post-infection *via* luminescence detection in living animals. Day 4 corresponds to the peak of RSV-luciferase replication in mice, as previously described [30]. We compared Viaskin®-N immunization to intra-nasal vaccination since our previous studies demonstrated that intra-nasal was the most efficient route for N-nanorings to afford viral protection upon RSV challenge in mice [11]. Mice vaccinated intranasally or with Viaskin®-N were completely protected against virus replication in lungs as compared to the control group

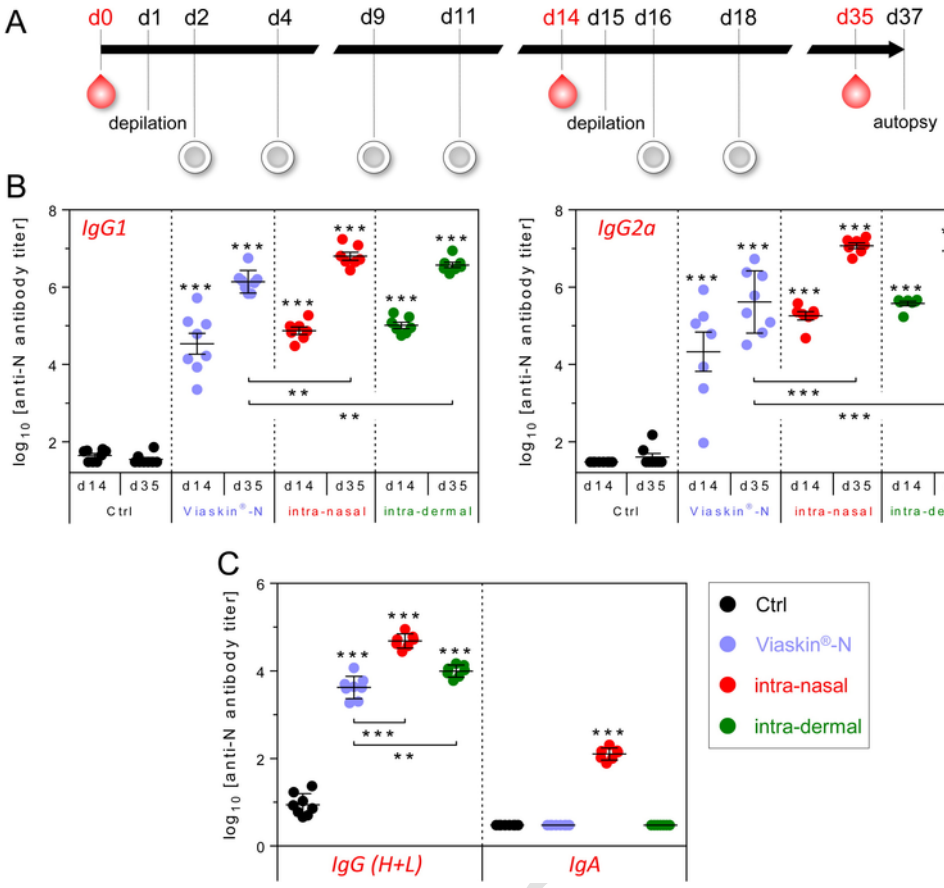

Fig. 3. Antibody responses induced by Viaskin®-N epicutaneous immunization protocol. (A) Six weeks BALB/c mice were immunized by epicutaneous application of Viaskin® loaded with 50 μg of N-nanorings and 25 μg of CpG ODN (Viaskin®-N). Viaskin®-N was applied for 48 h, 6 times, during 3 consecutive weeks as indicated. Blood samples were collected before the first immunization (day 0: d0) and at days 14 (d14) and 35 (d35) (schematized by red blood drops). As a positive control, mice were immunized with N-nanorings by intra-nasal (in red) or intra-dermal (in green) routes, twice at two weeks interval (day 4 and day 18). As a negative control, mice received 6 patches loaded with excipient alone (PBS) and 50 μg of CpG (Ctrl, in black). (B) N specific IgG1 (left panel) and IgG2a (right panel) were evaluated by indirect ELISA using N-nanorings as coating, in sera prepared from blood samples collected as described in panel (A). Data are mean ± SEM of individual antibody titers for each group (n = 7–8 per experimental group). (C) N specific IgG (H + L) and IgA were measured by indirect ELISA using N-rings as a coating, in BAL fluids collected at autopsy. Data are mean ± SEM of individual antibody titers for each group (n = 7–8 per experimental group). *P* values were determined according to the Mann-Whitney test (***, $P < 0.001$; ****, $P < 0.0001$). The level of significance measured between vaccinated groups was indicated above horizontal capped lines. The level of significance measured between each vaccinated groups and the negative control (Ctrl) group, at day 14 and day 35, was indicated above each histogram bar. (For interpretation of the references to color in this figure legend, the reader is referred to the web version of this article.)

($P < 0.0001$) (Fig. 6A). These results were further confirmed by the measure of luminescence in lung homogenates collected during the autopsy performed at day 5 post-infection (Fig. 6B) and by the measure of viral copy number by quantitative RT-PCR, performed from lung mRNA collected at day 5 post-infection (Fig. S4).

Control mice showed a slight reduction in body weight from day 4 to day 7 post-infection (significant at day 7 post-infection as compared to Viaskin®-N group, $P < 0.05$) that was not recorded in vaccinated animals (Fig. 6C). Of note, none of the animals, including in the control group, developed visible clinical symptoms. Overall, these results indicate that N-nanorings associated to CpG ODN and administered epicutaneously using Viaskin® patches gave rise to significant virological and clinical protections against RSV challenge.

3.5. Viaskin®-N epicutaneous vaccine induced limited neutrophil and eosinophil recruitment upon RSV infection, without exacerbating lung pathology

The analysis of the BAL cell composition, carried out at day 5 post-infection, revealed a similar neutrophil infiltration between the Viaskin®-N group and the control group (mean percentage of 23 ± 4% for the Viaskin®-N immunized group *versus* 16 ± 10% for the negative control group, $P = 0.4$) (Fig. 7A). Of note, the infiltration of neutrophils was significantly lower for the intra-nasal group (mean percentage of 8 ± 4%, $P < 0.01$). At this time-point, the proportion of eosinophils remained low in all group (mean percentage < 1%). At day 11 post infection, a lower infiltration of neutrophils was observed for the two vaccinated groups compared to the control group (mean percentage of 24 ± 12% for the control group *versus* 9 ± 6% for the Viaskin®-N group, $P < 0.05$ and 8 ± 3% for the intra-nasal group, $P < 0.05$). At this time-point, however, the Viaskin®-N group presented a slightly higher infiltration of eosinophils compared to the intra-nasal group and the control group (mean percentage of 3 ± 3% *versus* 0.3 ± 0.1% for the intra-nasal group, $P < 0.01$ and 0.8 ± 0.5% for the control group, $P = 0.1$). Of note, there were no significant differences in total cell count between the three groups at day 11 post-infection, indicating that cell percentages presented in Fig. 7A were well representative of the absolute number of each leukocyte population. In agreement with this observation, the concentration of pulmonary KC, TNF-α and eotaxin observed for the Viaskin®-N group were similar to those observed for the control group, but significantly higher to those measured in the intra-nasal

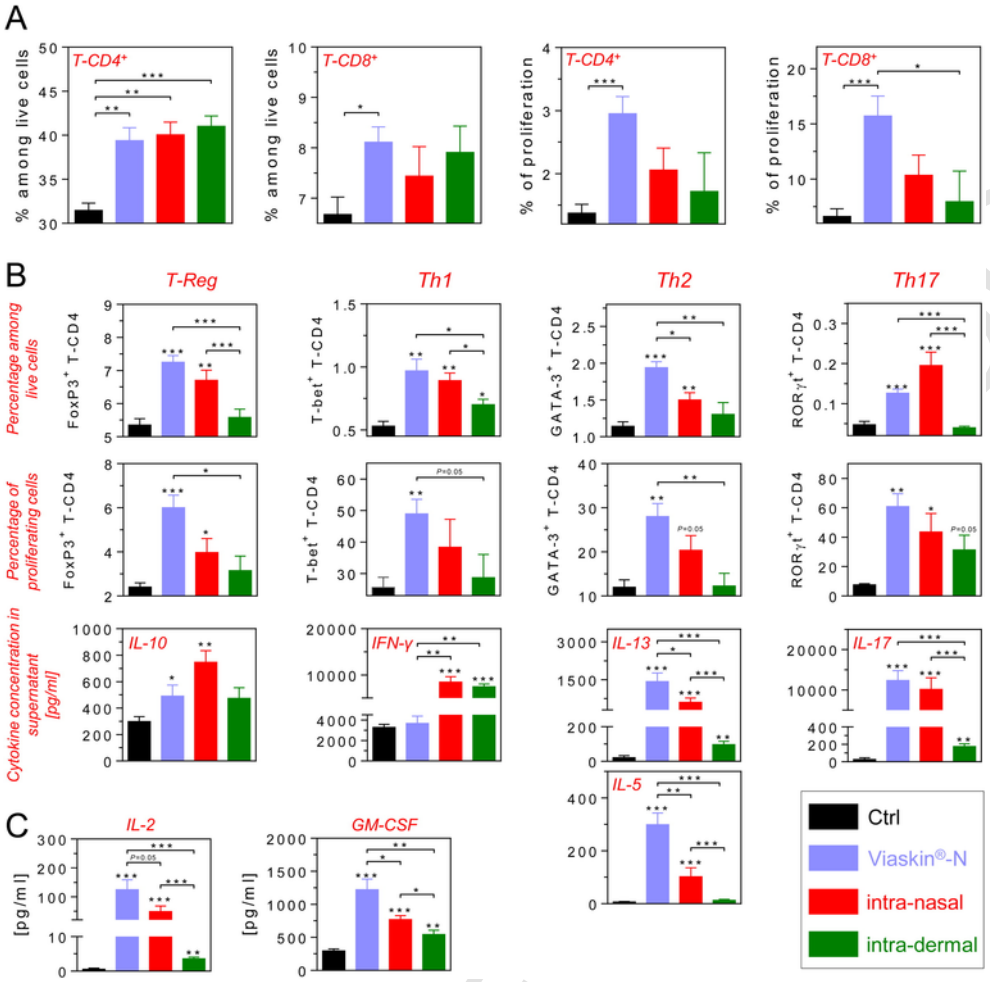

Fig. 4. Viaskin®-N epicutaneous immunization induces cellular responses in mice. BALB/c mice were epicutaneously immunized as described in Fig. 3. Splenocytes collected at autopsy (day 37) were labelled with CFSE and stimulated *in vitro* with N-nanorings (N) for 96 h at 37 °C + 5% CO_2. Then, cells were stained with anti-CD3, anti-CD4 and anti-CD8 antibodies conjugated to relevant fluorophore (A). Additionally, cells were stained intracellularly with anti-FoxP3, anti-T-bet, anti-GATA-3 and anti-RORγt antibodies conjugated to relevant fluorophores (B). Cells were analyzed using an LSR Fortessa cytometer. (B, bottom panels and C) Cell culture supernatants were collected after 48 h at 37 °C + 5% CO_2 and cytokine concentration was measured by multiplex analysis. Data are mean + SEM of individual concentration values for each group (n = 6–8 per experimental group). *P* values were determined according to the Mann-Whitney test (*, $P < 0.05$, **, $P < 0.01$, ***, $P < 0.001$). The level of significance measured between vaccinated groups was indicated above horizontal capped lines. The level of significance measured between each vaccinated groups and the negative control (Ctrl) group was indicated above each histogram bar.

group ($P < 0.05$ for KC concentration and $P < 0.01$ for TNF-α and eotaxin concentrations) (Fig. 7C). Furthermore, the level of inflammatory cytokines IL-1 Beta and IL-6 observed for the Viaskin®-N group was significantly higher to that measured for the intra-nasal group ($P < 0.05$ for IL-1 Beta concentration and $P < 0.01$ for IL-6 concentration). Additionally, the levels of monocyte-recruiting cytokines CCL-2 and CCL-7 and the levels of DC-recruiting cytokines CCL-4 and CXCL-10 were significantly higher to those observed for the intra-nasal group ($P < 0.01$ for CCL-2, $P < 0.05$ for CCL-7, $P < 0.01$ for CCL-4 and $P < 0.01$ for CXCL-10) (Fig. 7C). At first instance, these results could be interpreted as a slight exacerbation of lung inflammation and pathology after Viaskin®-N immunization. However, histological staining of the lung sections performed at day 11 post-infection did not revealed any signs of lung pathology or scar tissue, despite a slightly higher secretion of mucus in bronchioles for both vaccinated groups as compared to control group (Fig. 8). Moreover, the level of inflammatory cytokines induced after Viaskin®-N immunization was similar or even lower to that induced in the control group (Fig. 7). Overall, these data indicate that Viaskin®-N epicutaneous vaccine induces a limited lung inflammation upon RSV challenge that is not associated with lung injury.

3.6. RSV infection revealed the priming of Th1, Th17 and Treg responses upon Viaskin®-N epicutaneous vaccination

The levels of pulmonary Th1 (IFN-γ) and Th2 (IL-4, IL-13) cytokines observed for Viaskin®-N vaccinated mice at day 5 post-infection were similar to those observed for the control group ($P = 0.3$ for IFN-γ, $P = 0.7$ for IL-4 and $P = 0.8$ for IL-13) but significantly higher than those observed for the intra-nasal group ($P < 0.01$). On the other hand, the level of the Th1-associated cytokine IL12p70 was significantly higher in the Viaskin®-N group than in the control group ($P < 0.05$) and the intra-nasal group ($P < 0.01$). (Fig. 9, left panels). Of note, the level of these cytokines was also measured from lung samples collected at day 11 post-infection, but concentrations were low or undetectable for all groups. Additionally, the pulmonary concentrations of IL-17A and IL-23 were higher for the Viaskin®-N group ($P < 0.05$ *versus* the control group and $P < 0.01$ *versus* the in-

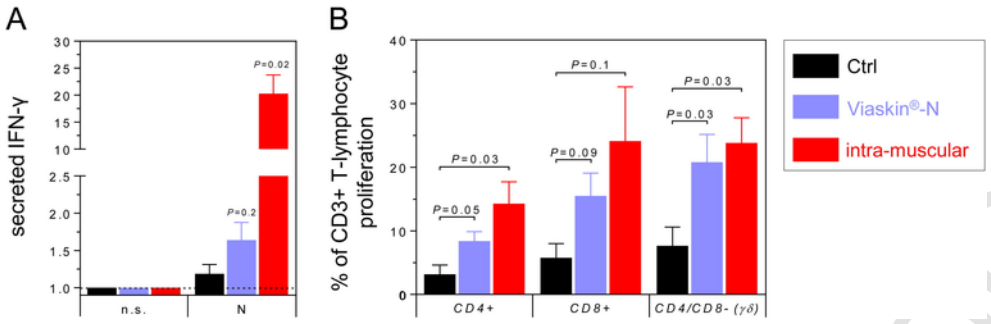

Fig. 5. Immunogenicity of Viaskin®-N epicutaneous vaccine in piglets. 8 weeks piglets were immunized with Viaskin® loaded with N-nanorings (100 μg) and CpG (100 μg) (Viaskin®-N, in blue) or CpG alone (100 μg) (Ctrl, in black). Immunization schedule was the same than the one used for mice experiments described in Fig. 3A. As a positive control, piglets were immunized by intra-muscular injection twice at two weeks interval with 20 μg of N-nanorings, adjuvanted with Montanide™ ISA 71 VG (intra-muscular, in red). Piglets splenocytes, collected 36 days after the first immunization, were labelled with CFSE and stimulated with Xvivo medium (negative control, non-stimulated: n.s.) or N-nanorings (N). (A) Cells were incubated 48 h at 37 °C and IFN-ϒ was measured from supernatant by sandwich ELISA. Data are expressed as individual fold increase of optical density (O.D.) at 450 nm over O.D. at 450 nm measured from supernatant collected from non-stimulated cells. (B) Cells were incubated for another 48 h at 37 °C + 5% CO2 and then stained with 7-AAD to exclude dead cells and with anti-CD3, anti-CD4 and anti-CD8 antibodies associated to relevant fluorophore-conjugated secondary antibodies. Cells were analyzed using an LSRFortessa cytometer. Data are expressed as the individual percentage of proliferation (decrease of CFSE signal) normalized to non-stimulated cells. n = 4–5 per experimental group and *P* values were determined according to the Mann-Whitney test (*, $P < 0.05$; **, $P < 0.01$). (For interpretation of the references to color in this figure legend, the reader is referred to the web version of this article.)

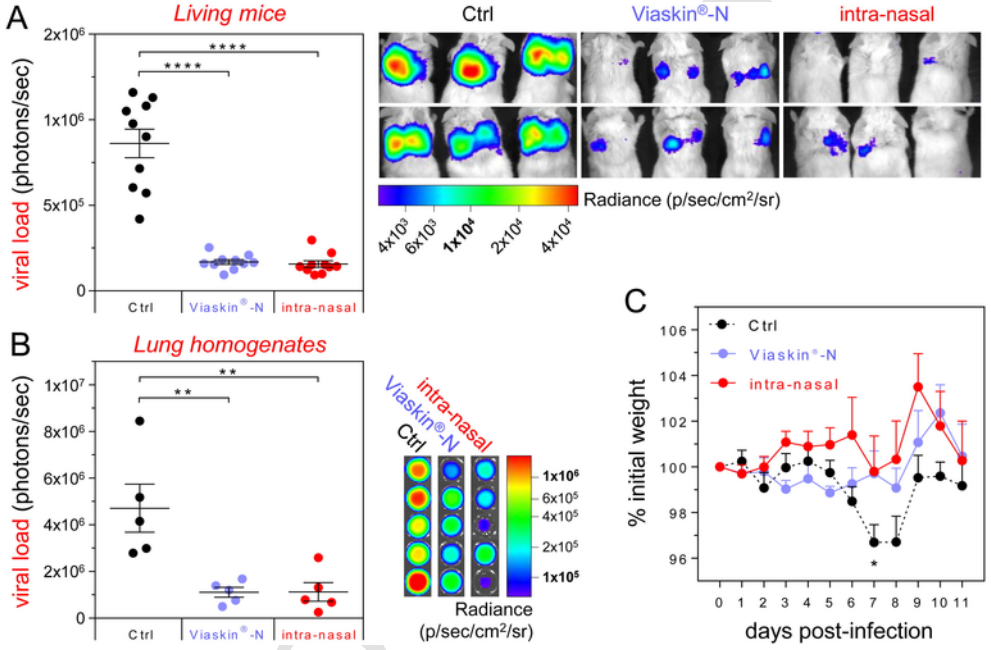

Fig. 6. Evaluation of the protective efficacy of Viaskin®-N against RSV infection in mice. BALB/c mice were immunized as described in Fig. 3. Three weeks after the last immunization (day 37, see Fig. 3A), mice were challenged with 8.8×10^4 PFU's of recombinant RSV-Luciferase. This recombinant virus allowed us to monitor virus replication in the lung of living mice, using luminescence detection as described in the material and methods. (A) Viral replication was evaluated in the lungs of living mice at day 4 post-infection (n = 10 per experimental group). As an illustration, a snapshot of the back of 6 representative mice of each group is shown on the right. (B) Viral replication was evaluated from lung homogenates collected at day 5 post-infection (n = 5 per experimental group). As an illustration, a photograph of each wells is shown on the right. Data are mean ± SEM of individual values expressed in photons per second. *P* values were determined according to the Mann-Whitney test (****, $P < 0.0001$; **, $P < 0.01$). (C) Body weight loss was monitored daily until day 11 post-infection. Body weight is expressed as % of initial weight at day 0. Data are mean + SEM of individual values (n = 10 per experimental group between day 0 and day 5 post-infection; n = 5 per experimental group between day 5 and day 11 post-infection). The significance of the differences observed between the control group (Ctrl, black dotted curves) and the Viaskin®-N group (blue line) at day 7 post-infection was evaluated according to the Mann-Whitney test (*, $P < 0.05$). (For interpretation of the references to color in this figure legend, the reader is referred to the web version of this article.)

tra-nasal group for IL-17 concentration) (Fig. 9). These results are consistent with the data obtained in spleen (Fig. 4), and is an indication of a Th17 immune orientation after Viaskin®-N epicutaneous immunization. This Th17 orientation could indeed explain the higher secretion of TNF-α and the slight increase in neutrophils recruitment observed in the Viaskin®-N group upon infection (Fig. 7A and B). A slight increase of IL-10 concentration was also observed in BAL for the Viaskin®-N group, suggesting that Viaskin®-N also induce an immuno-modulatory response in lung (Fig. 9, right panel). To confirm these results, the expression of IL-17 and FoxP3 was evaluated by quantitative RT-PCR for Viaskin®-N immunized mice and the control group using mRNA extracted from lungs collected at day 5 post infection. A significant increase of *IL-17* and *FoxP3* mRNA expression was measured compared to the control group (Fig. S5), confirming that Viaskin®-N also stimulated a Treg response in lung that might limit a potential RSV-induced immuno-pathology.

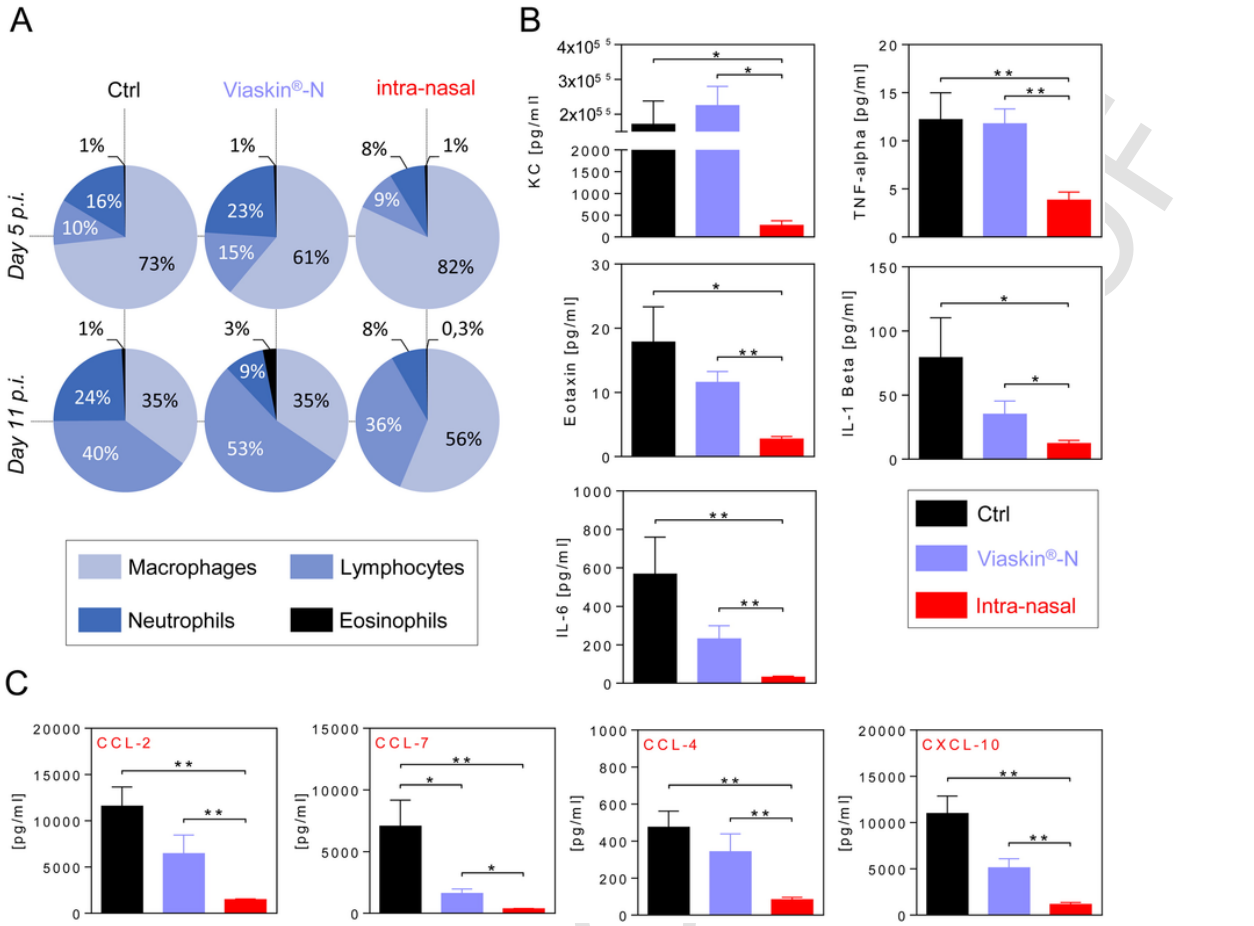

Fig. 7. Lung inflammation upon RSV challenge in Viaskin®-N vaccinated mice. BALB/c mice were immunized as described in Fig. 3 and challenged as described in Fig. 6. (A) BAL cells collected at day 5 or day 11 post-infection from individual mice were stained with May-Grünwald-Giemsa and leukocytes were counted. Percentage of each subset is represented by a pie chart for each immunized group. (B) The concentration of KC (GRO-α/CXCL-1) was determined from lung homogenates and the concentration TNF-alpha and Eotaxin were determined from BAL collected at day 5 post-infection by multiplex analysis. (C) The concentration of CCL-2, CCL-7, CCL-4 and CXCL-10 was determined from lung homogenates collected at day 5 post-infection by multiplex analysis. Data are mean + SEM of individual values (n = 5 per experimental group). *P* values were determined according to the Mann-Whitney test (*, $P < 0.05$; **, $P < 0.01$).

4. Discussion

The objective of the present study was the preclinical evaluation of a prophylactic epicutaneous vaccine against RSV that combines two innovative technologies: Viaskin® patches as an epicutaneous delivery platform on intact skin and RSV nucleoprotein nanorings (N-nanorings) as an antigen. In 2003, Godefroy et al. first demonstrated the feasibility of an epicutaneous vaccine against RSV in mice. In that study, authors used recombinant polypeptides containing a G protective epitope (G2Na), adjuvanted with cholera toxin (CT), applied by wetting on shaved skin [35]. However, although G2Na was able to give a significant level of protection against RSV challenge, specific antibody titers were low, highly heterogeneous and mostly of IgG1 isotype, indicating a Th2 orientation that may be associated to immuno-pathology and disease enhancement upon RSV challenge. Unfortunately, the effective presence of a vaccine-induced disease enhancement was not evaluated in that study.

In the present work, we demonstrated that Viaskin® patches loaded with N-nanorings and CpG ODN as adjuvant (Viaskin®-N) were immunogenic in mice and piglets, by potently priming N-specific memory CD4 and CD8 T-cells, as well as CD4/CD8 negative T-cells in piglets, *bona fide* γδ T-cells. As we mentioned in the introduction, the presence of this N-specific cellular response is a good indicator of vaccine efficacy since it has been correlated with viral protection in previous studies [11]. Moreover, CD8 T-cells are known to participate to viral clearance upon RSV infection in mice and human [36,37]. The effective role of γδ T-cells in the context of RSV infection is, however, poorly understood but they might participate in the reduction of RSV-associated immunopathology [38]. On, the other hand, anti-N humoral response, although it possesses no proven role in protection, was used here as an efficient marker for immunogenicity in mice. In piglets, however, it was not possible to observe any induction of antibody responses against N (data not shown). Interestingly, these results could be related to clinical data obtained by Combadière et al., showing a significant and selective increase of specific CD8 T-cells after transcutaneous immunization with inactivated influenza virus, without induction of neutralizing antibodies [39]. In agreement with our data, these results suggests an intrinsic defect of Langerhans cells (LC)-mediated immune response to induced a humoral response, as previously observed *in vitro* for human LC [40]. However, some patches formulations (adjuvant) or therapeutic schemes (number of application) might be able to overcome this limitation as observed in mice study [41]. In mice, indeed, our Vi-

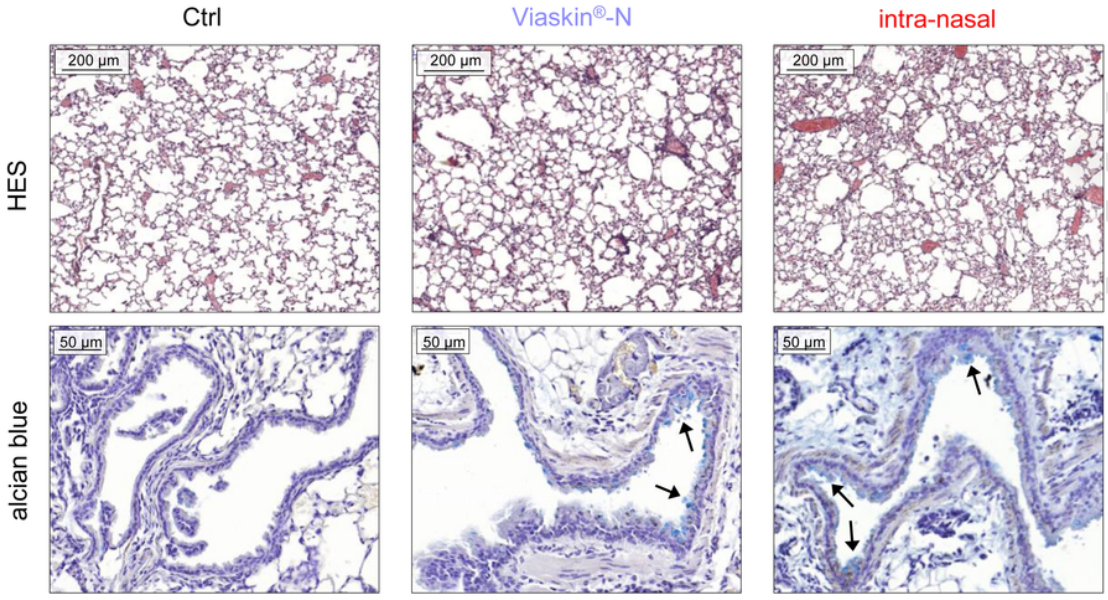

Fig. 8. Histological analysis of lung upon RSV challenge in Viaskin®-N vaccinated mice. BALB/c mice were immunized as described in Fig. 3 and challenged as described in Fig. 6. Lungs collected at day 11 post-infection were fixed in PBS-PFA, embedded in paraffin and sliced. Lung sections were colored using Hematoxylin Eosin Safran (HES) or alcian blue and images were acquired using slide scanner. The presence of mucus is indicated by black arrows. (For interpretation of the references to color in this figure legend, the reader is referred to the web version of this article.)

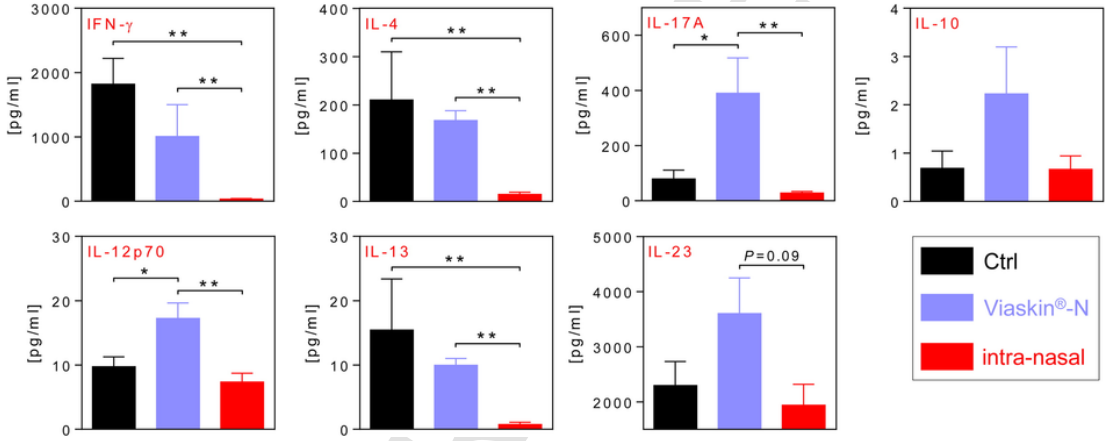

Fig. 9. Viaskin®-N immunization promoted a local Th1/Th17 oriented immune response upon RSV challenge. BALB/c mice were immunized as described in Fig. 3 and challenged as described in Fig. 6. The level of IFN-γ, IL-5, IL-13, IL-12p70, IL-17 and IL-23 cytokines was determined from lung homogenates collected at day 5 post-infection and the level of IL-10 was determined from BAL collected at day 5 post-infection, by multiplex analysis. Data are mean + SEM of individual values (n = 5 per experimental group). *P* values were determined according to the Mann-Whitney test (*, $P < 0.05$; **, $P < 0.01$).

askin®-N epicutaneous vaccine induced a well-balanced IgG1/IgG2a specific antibody response and primed Th1 CD4 T-cells. Of note, this Th1 orientation observed after epicutaneous vaccination was less marked than for intra-nasal and intra-dermal immunizations. The use of CpG ODN as an adjuvant probably contributed to this Th1 orientation. Indeed, CpG ODN possesses an intrinsic capacity to drive the immune response toward the Th1 phenotype, *via* triggering TLR9 pathway in antigen-presenting cells (APC) [42]. We chose CpG ODN as an adjuvant based on our previously published data, showing that the addition of CpG ODN to N-nanorings administered intranasally in neonate mice helped to prevent the Th2 bias of the recall response and reduced the eosinophilic reaction observed upon RSV challenge [33]. This choice was further supported by other studies demonstrating that CpG ODN used as an adjuvant in transcutaneous vaccine approaches was able to increase vaccine immunogenicity and the differentiation of specific Th1 cells [43–45]. Importantly, CpG ODN has been demonstrated as a safe and well tolerated adjuvant in a phase 1 clinical trial of an HBV vaccine in HIV-seropositive adults [46].

Remarkably, Viaskin®-N epicutaneous vaccine also primed CD4 T-lymphocytes from the RORγt$^+$ (Th17) and the FoxP3$^+$ regulatory cell (Tregs) subsets in mice. These Th17 and Tregs were identified in splenocytes upon antigen-specific stimulation and locally in the lung upon RSV infection. The role of the Th17 response in the physiopathology of RSV infection still remains controversial. Indeed, Th17 response seems to possess a bit of duplicity in the context of RSV infection. On the one hand, numerous studies suggest that the Th17 response would be beneficial in some cases of RSV infection [47]. For example, local IL-17 production might accelerate recovery of RSV infection in non-ventilated patients [48]. On the other hand, an exacerbated Th17 response might be responsible for acute inflammation and pathology notably by promoting the production of

chemokines such as KC, CCL20 (MIP-3α) and IL-6 by stromal cells which then promote neutrophil recruitment to the lung [47]. The stimulation of a Th17 response by Viaskin®-N could indeed explain our findings showing a slight increase of neutrophils recruitment and a significant increase of TNF-α secretion in the lung upon RSV challenge. However, in our case, this Th17 response was not associated with disease exacerbation upon challenge. Indeed, Viaskin®-N vaccinated mice presented an inflammatory cytokine production pattern in the lung that was similar to that observed for the control group upon RSV challenge. Additionally, Viaskin®-N vaccinated mice were totally protected from RSV replication in the lung, which is the main site of infection, without any weight loss, clinical symptoms or signs of lung injury. Of note, we used an immunogen dose and an immunization schedule that was optimal to afford viral protection in the lung. Indeed, a significant increase of pulmonary viral load was observed when the number of Viaskin®-N application was decrease twofold (*i.e.* one patch per week instead of two) (Fig. S4). However, viral protection was still significant compared to the control group ($P < 0.05$).

Indeed, the degree of pulmonary disease caused by RSV infection is highly dependent on a fine regulation between pro-inflammatory and regulatory immune responses [49]. Tregs has especially been shown to efficiently hang in this balance by inhibiting Th2 associated immune responses and by limiting eosinophils infiltration in the lung upon RSV infection that are the primary cause of RSV-induced lung immunopathology [50,51]. More specifically, the importance of Treg/Th17 balance in the pathogenesis of RSV infection has been highlighted [49]. Indeed, it has been shown that the percentage of Tregs and the levels of IL-10 and TGF-β were significantly lower in infants suffering from RSV bronchiolitis than in non-RSV pneumonia-suffering or healthy infants [52]. Conversely, the percentage of Th17 and the level of IL-17 was found higher in these RSV bronchiolitis-suffering individuals. Moreover, Treg and Th17 populations seems closely interconnected since differentiation of Tregs into Th17 have been recorded in a previous experiment [53]. In our case, the stimulation of Treg by Viaskin®-N vaccination might therefore prevents from a deleterious Th17 immune response and explain the absence of detectable macroscopic and microscopic pathology upon challenge. In fact, the capacity of Viaskin®-N to stimulate Treg response could be linked to the Viaskin® platform itself that has been initially designed to induce tolerance to allergens. Indeed, our previous studies demonstrated that allergens applied on intact skin with Viaskin® patches efficiently promote a down-modulation of specific immune response in sensitized mice in association with the induction of Tregs [16,20,21]. This unique particularity could be related to the unique targeting of LC [21], mainly described to promote regulatory T cell responses [54,55]. This tolerogenic immune-modulation could be obtained only when the antigen is administered on intact skin [19]. In human, LC have also been shown to maintained the Treg pool [55] but also, in agreement with our data, to preferentially induce Th17 responses [56]. Originally, Viaskin®-N epicutaneous vaccine would advantageously combine the induction a protective immunity against RSV replication to the avoidance of the Th2-mediated vaccine enhance disease that could occurs upon RSV challenge [3], by the induction of immuno-modulatory T-cell.

In piglets, we demonstrated that Viaskin® patches were able to promote the passage of N-nanorings fused to GFP (N-GFP) to the epidermis, resulting in an efficient capture of N-GFP by LC. Bearing in mind the similarity between swine and human skin, a similar uptake of N-nanorings by LC could be expected in human. Therefore, these results are really encouraging, especially with regards to the feasibility of Viaskin® vaccination in human.

Our recent data demonstrated that N-nanorings can be used as a potent vaccine carrier for heterologous antigens such as influenza M2 ectodomain (M2e) [29]. In light of these results, we undertook to fuse a neutralizing epitope derived from RSV F protein to N. Such chimeric N-nanorings (N-Fe) would present the advantage to combine a potent cellular response (afforded by N) to a neutralizing antibody response (afforded by the F epitope). These N-Fe are still under optimization for their use in combination with Viaskin® patches. For now, the evaluation of their antigenicity and their protective potency in mice using "conventional" immunization routes has given interesting results [57].

Very recently, Gavillet et al. demonstrated that a single application of Viaskin® patches loaded with detoxified pertussis toxin and/or pertactin and filamentous hemagglutinin, without adjuvant, was efficient to reactivate vaccine-induced pertussis immunity in mice and to protect mice against a *B. pertussis* challenge [23]. Furthermore, this booster vaccine candidate will soon be tested in a phase I clinical trial. These promising results raised a great deal of hope concerning the use of Viaskin® patches as a non-invasive vaccine delivery method. Combined to our present results, these data also highlighted the potential versatility of the Viaskin® platform.

Besides immunological aspects Viaskin®-N epicutaneous vaccine would presents several advantages compared to other vaccine candidates. First, the immunization protocol is needle free and, unlike other transcutaneous vaccines, does not require skin preparation before application. Therefore, this painless vaccine may have a better acceptability for the vaccination of sensible population such as young children. Secondly, this easy-to-use and potentially self-applicative vaccination method is expected to overcome some issues associated with injectable vaccinations such as the need of sterile medical devices and skilled health-care professionals or the requirement of stringent store conditions and the maintenance of cold-chain. Paradoxically, these issues are especially marked in developing countries where RSV infections constitute the most serious burden [58].

5. Conclusion

In the present study, we demonstrated the feasibility of an epicutaneous RSV vaccine using Viaskin® patches. The unique properties of Viaskin® epicutaneous patches permitted to efficiently protect mice against RSV replication, while actively avoiding RSV-associated lung immuno-pathology by the stimulation of Treg response. Importantly, the significant level of protection obtained in the lung suggest that Viaskin®-N vaccine would prevent bronchiolitis and pneumonia, the most severe clinical manifestations of RSV infection triggered by the virus replication in the deep respiratory tract. In addition, Viaskin® patches as a non-invasive vaccine platform might be particularly suitable for the vaccination of young children. Overall, Viaskin® patches combined to N-nanorings would constitute a pertinent and promising vaccine strategy against RSV. From these results and those obtained with *B. pertussis* [23], it becomes apparent that the Viaskin® patch constitutes an effective vaccine device for the development of innovative and non-invasive prophylactic treatments against pathogens.

Supplementary data to this article can be found online at http://dx.doi.org/10.1016/j.jconrel.2016.10.003.

Funding

This work was supported by the French national research agency "Agence Nationale de la Recherche" [ANR-12-RPIB-0004-02].

Conflicts of interest

The authors declare that there are no conflicts of interest.

Acknowledgments

We thank Jérôme Pottier, Mathilde Beauducel, Marlène Héry and Charline Pontlevoy from the Fish and Rodent Experimental Infectiology unit (IERP, INRA, Jouy-en-Josas, France), for their support in the animal facilities. We thank Thierry Chaumeil, Maud Renouard and Edouard Guitton from the Experimental Infectiology Platform (PFIE, INRA, Nouzilly, France) for their support in performing piglet experiments. We thank the MIMA2 platform for access to the IVIS-200, which was financed by the Ile de France region (SESAME). We also thank Nathalie Donne for the coordination of this project.

References

[1] R. Rodriguez, O. Ramilo, Respiratory syncytial virus: how, why and what to do, J. Infect. 68 (Suppl 1) (2014) S115–S118, http://dx.doi.org/10.1016/j.jinf.2013.09.021.

[2] M.F. Delgado, S. Coviello, A.C. Monsalvo, G.A. Melendi, J. Zea Hernandez, J.P. Batalle, L. Diaz, A. Trento, H.-Y. Chang, W. Mitzner, J. Ravetch, J.A. Melero, P.M. Irusta, F.P. Polack, Lack of antibody affinity maturation due to poor Toll-like receptor stimulation leads to enhanced respiratory syncytial virus disease, Nat. Med. 15 (2009) 34–41.

[3] P.L. Collins, J.A. Melero, Progress in understanding and controlling respiratory syncytial virus: still crazy after all these years, Virus Res. 162 (2011) 80–99, http://dx.doi.org/10.1016/j.virusres.2011.09.020.Progress.

[4] B.S. Graham, K. Modjarrad, J.S. McLellan, Novel antigens for RSV vaccines, Curr. Opin. Immunol. 35 (2015) 30–38, http://dx.doi.org/10.1016/j.coi.2015.04.005.

[5] T.G. Morrison, E.E. Walsh, Subunit and virus-like particle vaccine approaches for respiratory syncytial virus, Curr. Top. Microbiol. Immunol. 372 (2013) 285–306.

[6] C.-A. Siegrist, L. Mondoulet, Method of Vaccination — WO2011/128430, in: https://patentscope.wipo.int/search/en/detail.jsf?docId=WO2011128430&recNum=137&docAn=EP2011055991&queryString=%2522streptococcus%2520pneumoniae%2522&maxRec=6375, 2011 (accessed February 8, 2016).

[7] J.-F. Eleouët, S. Riffault, N Protein Fusion Proteins of a Virus in the Paramyxoviridae-Protein of Interest Family — WO/2007/119011, in: https://patentscope.wipo.int/search/en/detail.jsf?docId=WO2007119011, 2007 (accessed February 8, 2016).

[8] J.-F. Eleouët, S. Riffault, Preparation of Soluble N-protein/truncated P-protein Complexes or N-proteins Soluble in a Virus of the Paramyxoviridae Family and Use Thereof in Vaccines — WO/2006/117456, in: https://patentscope.wipo.int/search/en/detail.jsf?docId=WO2006117456, 2006 (accessed February 8, 2016).

[9] T.-L. Tran, N. Castagné, D. Bhella, P.F. Varela, J. Bernard, S. Chilmonczyk, S. Berkenkamp, V. Benhamo, K. Grznarova, J. Grosclaude, C. Nespoulos, F.A. Rey, J.-F. Eléouët, The nine C-terminal amino acids of the respiratory syncytial virus protein P are necessary and sufficient for binding to ribonucleoprotein complexes in which six ribonucleotides are contacted per N protein protomer, J. Gen. Virol. 88 (2007) 196–206, http://dx.doi.org/10.1099/vir.0.82282-0.

[10] R.G. Tawar, S. Duquerroy, C. Vonrhein, P.F. Varela, L. Damier-Piolle, N. Castagné, K. MacLellan, H. Bedouelle, G. Bricogne, D. Bhella, J.-F. Eléouët, F.A. Rey, Crystal structure of a nucleocapsid-like nucleoprotein-RNA complex of respiratory syncytial virus, Science (80-.) 326 (2009) 1279–1283, http://dx.doi.org/10.1126/science.1177634.

[11] X. Roux, C. Dubuquoy, G. Durand, T.-L. Tran-Tolla, N. Castagné, J. Bernard, A. Petit-Camurdan, J.-F. Eléouët, S. Riffault, Sub-nucleocapsid nanoparticles: a nasal vaccine against respiratory syncytial virus, PLoS One 3 (2008)e1766http://dx.doi.org/10.1371/journal.pone.0001766.

[12] K. Blodörn, S. Hägglund, J. Fix, C. Dubuquoy, B. Makabi-Panzu, M. Thom, P. Karlsson, J.-L. Roque, E. Karlstam, J. Pringle, J.-F. Eléouët, S. Riffault, G. Taylor, J.F. Valarcher, Vaccine safety and efficacy evaluation of a recombinant bovine respiratory syncytial virus (BRSV) with deletion of the SH gene and subunit vaccines based on recombinant human RSV proteins: N-nanorings, P and M2-1, in calves with maternal antibodies, PLoS One 9 (2014)e100392http://dx.doi.org/10.1371/journal.pone.0100392.

[13] I.M. Belyakov, S.A. Hammond, J.D. Ahlers, G.M. Glenn, J.A. Berzofsky, Transcutaneous immunization induces mucosal CTLs and protective immunity by migration of primed skin dendritic cells, J. Clin. Invest. 113 (2004) 998–1007, http://dx.doi.org/10.1172/JCI20261.

[14] J.A. Mikszta, P.E. Laurent, Cutaneous delivery of prophylactic and therapeutic vaccines: historical perspective and future outlook, Expert Rev. Vaccines 7 (2008) 1329–1339, http://dx.doi.org/10.1586/14760584.7.9.1329.

[15] H.J.H.B. Hirschberg, E. van Riet, D. Oosterhoff, J.A. Bouwstra, G.F.A. Kersten, Animal models for cutaneous vaccine delivery, Eur. J. Pharm. Sci. 71 (2015) 112–122, http://dx.doi.org/10.1016/j.ejps.2015.02.005.

[16] L. Mondoulet, V. Dioszeghy, M. Ligouis, V. Dhelft, C. Dupont, P.-H. Benhamou, Epicutaneous immunotherapy on intact skin using a new delivery system in a murine model of allergy, Clin. Exp. Allergy 40 (2010) 659–667, http://dx.doi.org/10.1111/j.1365-2222.2009.03430.x.

[17] L. Mondoulet, V. Dioszeghy, T. Larcher, M. Ligouis, V. Dhelft, E. Puteaux, Y. Cherel, F. Letourneur, C. Dupont, P.-H. Benhamou, Epicutaneous immunotherapy (EPIT) blocks the allergic esophago-gastro-enteropathy induced by sustained oral exposure to peanuts in sensitized mice, PLoS One 7 (2012)e31967http://dx.doi.org/10.1371/journal.pone.0031967.

[18] L. Mondoulet, V. Dioszeghy, M. Ligouis, V. Dhelft, E. Puteaux, C. Dupont, P.-H. Benhamou, Epicutaneous immunotherapy compared with sublingual immunotherapy in mice sensitized to pollen (Phleum pratense), ISRN Allergy 2012 (2012) 375735, http://dx.doi.org/10.5402/2012/375735.

[19] L. Mondoulet, V. Dioszeghy, E. Puteaux, M. Ligouis, V. Dhelft, F. Letourneur, C. Dupont, P.-H. Benhamou, Intact skin and not stripped skin is crucial for the safety and efficacy of peanut epicutaneous immunotherapy (EPIT) in mice, Clin. Transl. Allergy 2 (2012) 22, http://dx.doi.org/10.1186/2045-7022-2-22.

[20] V. Dioszeghy, L. Mondoulet, V. Dhelft, M. Ligouis, E. Puteaux, C. Dupont, P.-H. Benhamou, The regulatory T cells induction by epicutaneous immunotherapy is sustained and mediates long-term protection from eosinophilic disorders in peanut-sensitized mice, Clin. Exp. Allergy 44 (2014) 867–881, http://dx.doi.org/10.1111/cea.12312.

[21] V. Dioszeghy, L. Mondoulet, V. Dhelft, M. Ligouis, E. Puteaux, P.-H. Benhamou, C. Dupont, Epicutaneous immunotherapy results in rapid allergen uptake by dendritic cells through intact skin and downregulates the allergen-specific response in sensitized mice, J. Immunol. 186 (2011) 5629–5637, http://dx.doi.org/10.4049/jimmunol.1003134.

[22] L. Mondoulet, V. Dioszeghy, E. Puteaux, M. Ligouis, V. Dhelft, C. Plaquet, C. Dupont, P.-H. Benhamou, Specific epicutaneous immunotherapy prevents sensitization to new allergens in a murine model, J. Allergy Clin. Immunol. 135 (2015) http://dx.doi.org/10.1016/j.jaci.2014.11.028 (1546–57.e4).

[23] B.M. Gavillet, L. Mondoulet, V. Dhelft, C.S. Eberhardt, F. Auderset, H.T. Pham, J. Petre, P.-H. Lambert, P.-H. Benhamou, C.-A. Siegrist, Needle-free and adjuvant-free epicutaneous boosting of pertussis immunity: preclinical proof of concept, Vaccine 33 (2015) 3450–3455, http://dx.doi.org/10.1016/j.vaccine.2015.05.089.

[24] B. Malissen, S. Tamoutounour, S. Henri, The origins and functions of dendritic cells and macrophages in the skin, Nat. Rev. Immunol. 14 (2014) 417–428, http://dx.doi.org/10.1038/nri3683.

[25] F. Marquet, M. Bonneau, F. Pascale, C. Urien, C. Kang, I. Schwartz-Cornil, N. Bertho, Characterization of dendritic cells subpopulations in skin and afferent lymph in the swine model, PLoS One 6 (2011)e16320http://dx.doi.org/10.1371/journal.pone.0016320.

[26] F. Marquet, T.-P.V. Manh, P. Maisonnasse, J. Elhmouzi-Younes, C. Urien, E. Bouguyon, L. Jouneau, M. Bourge, G. Simon, A. Ezquerra, J. Lecardonnel, M. Bonneau, M. Dalod, I. Schwartz-Cornil, N. Bertho, Pig skin includes dendritic cell subsets transcriptomically related to human CD1a and CD14 dendritic cells presenting different migrating behaviors and T cell activation capacities, J. Immunol. 193 (2014) 5883–5893, http://dx.doi.org/10.4049/jimmunol.1303150.

[27] F.P. Schmook, J.G. Meingassner, A. Billich, Comparison of human skin or epidermis models with human and animal skin in in-vitro percutaneous absorption, Int. J. Pharm. 215 (2001) 51–56, http://dx.doi.org/10.1016/S0378-5173(00)00665-7.

[28] N. Castagne, A. Barbier, J. Bernard, H. Rezaei, J. Huet, C. Henry, B. Da Costa, J.-F. Eléouët, Biochemical characterization of the respiratory syncytial virus P-P and P-N protein complexes and localization of the P protein oligomerization domain, J. Gen. Virol. 85 (2004) 1643–1653, http://dx.doi.org/10.1099/vir.0.79830-0.

[29] P.-L. Hervé, M. Raliou, C. Bourdieu, C. Dubuquoy, A. Petit-Camurdan, N. Bertho, J.-F. Eléouët, C. Chevalier, S. Riffault, A novel subnucleocapsid nanoplatform for mucosal vaccination against influenza virus that targets the ectodomain of matrix protein 2, J. Virol. 88 (2014) 325–338, http://dx.doi.org/10.1128/JVI.01141-13.

[30] M.-A. Rameix-Welti, R. Le Goffic, P.-L. Hervé, J. Sourimant, A. Rémot, S. Riffault, Q. Yu, M. Galloux, E. Gault, J.-F. Eléouët, Visualizing the replication of respiratory syncytial virus in cells and in living mice, Nat. Commun. 5 (2014) 5104, http://dx.doi.org/10.1038/ncomms6104.

[31] D. Tudor, S. Riffault, C. Carrat, F. Lefèvre, M. Bernoin, B. Charley, Type I IFN modulates the immune response induced by DNA vaccination to pseudorabies virus glycoprotein C, Virology 286 (2001) 197–205, http://dx.doi.org/10.1006/viro.2001.0957.
[32] I. Schwartz-Cornil, M. Epardaud, M. Bonneau, Cervical duct cannulation in sheep for collection of afferent lymph dendritic cells from head tissues, Nat. Protoc. 1 (2006) 874–879, http://dx.doi.org/10.1038/nprot.2006.147.
[33] A. Remot, X. Roux, C. Dubuquoy, J. Fix, S. Bouet, M. Moudjou, J.-F. Eléouët, S. Riffault, A. Petit-Camurdan, Nucleoprotein nanostructures combined with adjuvants adapted to the neonatal immune context: a candidate mucosal RSV vaccine, PLoS One 7 (2012)e37722http://dx.doi.org/10.1371/journal.pone.0037722.
[34] O. Boyman, J. Sprent, The role of interleukin-2 during homeostasis and activation of the immune system, Nat. Rev. Immunol. 12 (2012) 180–190, http://dx.doi.org/10.1038/nri3156.
[35] S. Godefroy, L. Goestch, H. Plotnicky-Gilquin, T. Ngoc Nguyen, D. Schmitt, M.-J. Staquet, N. Corvaıä, Immunization onto shaved skin with a bacterial enterotoxin adjuvant protects mice against Respiratory Syncytial Virus (RSV), Vaccine 21 (2003) 1665–1671, http://dx.doi.org/10.1016/S0264-410X(02)00733-8.
[36] B.S. Graham, Biological challenges and technological opportunities for RSV vaccine development, Immunol. Rev. 239 (2011) 149–166, http://dx.doi.org/10.1111/j.1600-065X.2010.00972.x.Biological.
[37] G. Taylor, L.H. Thomas, S.G. Wyld, J. Furze, P. Sopp, C.J. Howard, Role of T-lymphocyte subsets in recovery from respiratory syncytial virus infection in calves, J. Virol. 69 (1995) 6658–6664. http://www.pubmedcentral.nih.gov/articlerender.fcgi?artid=189575&tool=pmcentrez&rendertype=abstract (accessed February 10, 2016).
[38] M. Aoyagi, N. Shimojo, K. Sekine, T. Nishimuta, Y. Kohno, Respiratory syncytial virus infection suppresses IFN-gamma production of gammadelta T cells, Clin. Exp. Immunol. 131 (2003) 312–317. http://www.pubmedcentral.nih.gov/articlerender.fcgi?artid=1808627&tool=pmcentrez&rendertype=abstract (accessed February 10, 2016).
[39] B. Combadière, A. Vogt, B. Mahé, D. Costagliola, S. Hadam, O. Bonduelle, W. Sterry, S. Staszewski, H. Schaefer, S. van der Werf, C. Katlama, B. Autran, U. Blume-Peytavi, Preferential amplification of CD8 effector-T cells after transcutaneous application of an inactivated influenza vaccine: a randomized phase I trial, PLoS One 5 (2010)e10818http://dx.doi.org/10.1371/journal.pone.0010818.
[40] E. Klechevsky, R. Morita, M. Liu, Y. Cao, S. Coquery, L. Thompson-Snipes, F. Briere, D. Chaussabel, G. Zurawski, A.K. Palucka, Y. Reiter, J. Banchereau, H. Ueno, Functional specializations of human epidermal Langerhans cells and $CD14^+$ dermal dendritic cells, Immunity 29 (2008) 497–510, http://dx.doi.org/10.1016/j.immuni.2008.07.013.
[41] T. Ouchi, A. Kubo, M. Yokouchi, T. Adachi, T. Kobayashi, D.Y. Kitashima, H. Fujii, B.E. Clausen, S. Koyasu, M. Amagai, K. Nagao, Langerhans cell antigen capture through tight junctions confers preemptive immunity in experimental staphylococcal scalded skin syndrome, J. Exp. Med. 208 (2011) 2607–2613, http://dx.doi.org/10.1084/jem.20111718.
[42] C. Bode, G. Zhao, F. Steinhagen, T. Kinjo, D.M. Klinman, CpG DNA as a vaccine adjuvant, Expert Rev. Vaccines. 10 (2011) 499–511, http://dx.doi.org/10.1586/erv.10.174.
[43] D.K. Hickey, F.E. Aldwell, K.W. Beagley, Transcutaneous immunization with a novel lipid-based adjuvant protects against Chlamydia genital and respiratory infections, Vaccine 27 (2009) 6217–6225, http://dx.doi.org/10.1016/j.vaccine.2009.08.001.
[44] D.K. Hickey, F.E. Aldwell, Z.Y. Tan, S. Bao, K.W. Beagley, Transcutaneous immunization with novel lipid-based adjuvants induces protection against gastric Helicobacter pylori infection, Vaccine 27 (2009) 6983–6990, http://dx.doi.org/10.1016/j.vaccine.2009.09.078.
[45] Y. Qiu, L. Guo, S. Zhang, B. Xu, Y. Gao, Y. Hu, J. Hou, B. Bai, H. Shen, P. Mao, DNA-based vaccination against hepatitis B virus using dissolving microneedle arrays adjuvanted by cationic liposomes and CpG ODN, Drug Deliv. 30 (2015) 1–8, http://dx.doi.org/10.3109/10717544.2014.992497.
[46] C.L. Cooper, J.B. Angel, I. Seguin, H.L. Davis, D.W. Cameron, CPG 7909 adjuvant plus hepatitis B virus vaccination in HIV-infected adults achieves long-term seroprotection for up to 5 years, Clin. Infect. Dis. 46 (2008) 1310–1314, http://dx.doi.org/10.1086/533467.
[47] J. Bystrom, N. Al-Adhoubi, M. Al-Bogami, A.S. Jawad, R.A. Mageed, Th17 lymphocytes in respiratory syncytial virus infection, Viruses 5 (2013) 777–791, http://dx.doi.org/10.3390/v5030777.
[48] T.E. Faber, H. Groen, M. Welfing, K.J.G. Jansen, L.J. Bont, Specific increase in local IL-17 production during recovery from primary RSV bronchiolitis, J. Med. Virol. 84 (2012) 1084–1088, http://dx.doi.org/10.1002/jmv.23291.
[49] T. Mangodt, M.A. Van Herck, S. Nullens, J. Ramet, J.J. De Dooy, P.G. Jorens, B.Y. De Winter, The role of Th17 and Treg responses in the pathogenesis of RSV infection, Pediatr. Res. 78 (2015) 483–491, http://dx.doi.org/10.1038/pr.2015.143.
[50] L.R. Durant, S. Makris, C.M. Voorburg, J. Loebbermann, C. Johansson, P.J.M. Openshaw, Regulatory T cells prevent Th2 immune responses and pulmonary eosinophilia during respiratory syncytial virus infection in mice, J. Virol. 87 (2013) 10946–10954, http://dx.doi.org/10.1128/JVI.01295-13.
[51] R.B. Fulton, D.K. Meyerholz, S.M. Varga, $Foxp3^+$ CD4 regulatory T cells limit pulmonary immunopathology by modulating the CD8 T cell response during respiratory syncytial virus infection, J. Immunol. 185 (2010) 2382–2392, http://dx.doi.org/10.4049/jimmunol.1000423.
[52] B. Li, F. Wu, X. Feng, D. Sun, Q. Cui, Z. Zhao, Changes and the clinical significance of $CD4^+$ $CD25^+$ regulatory T cells and Th17 cells in peripheral blood of infants with respiratory syncytial virus bronchiolitis, Chinese J. Cell. Mol. Immunol. 28 (2012) 426–428.
[53] H.J.P.M. Koenen, R.L. Smeets, P.M. Vink, E. van Rijssen, A.M.H. Boots, I. Joosten, Human CD25highFoxp3pos regulatory T cells differentiate into IL-17-producing cells, Blood 112 (2008) 2340–2352, http://dx.doi.org/10.1182/blood-2008-01-133967.
[54] M. Gomez de Agüero, M. Vocanson, F. Hacini-Rachinel, M. Taillardet, T. Sparwasser, A. Kissenpfennig, B. Malissen, D. Kaiserlian, B. Dubois, Langerhans cells protect from allergic contact dermatitis in mice by tolerizing CD8(+) T cells and activating Foxp3(+) regulatory T cells, J. Clin. Invest. 122 (2012) 1700–1711, http://dx.doi.org/10.1172/JCI59725.
[55] J. Seneschal, R.A. Clark, A. Gehad, C.M. Baecher-Allan, T.S. Kupper, Human epidermal Langerhans cells maintain immune homeostasis in skin by activating skin resident regulatory T cells, Immunity 36 (2012) 873–884, http://dx.doi.org/10.1016/j.immuni.2012.03.018.
[56] A.R. Mathers, B.M. Janelsins, J.P. Rubin, O.A. Tkacheva, W.J. Shufesky, S.C. Watkins, A.E. Morelli, A.T. Larregina, Differential capability of human cutaneous dendritic cell subsets to initiate Th17 responses, J. Immunol. 182 (2009) 921–933, http://dx.doi.org/10.4049/jimmunol.182.2.921.
[57] P.-L. Hervé, C. Deloizy, D. Descamps, M.-A. Rameix-Welti, J. Fix, J.S. Mclellan, J.-F. Eleouët, S. Riffault, RSV N-nanorings fused to palivizumab-targeted neutralizing epitope as a nanoparticle RSV vaccine, Nanomedicine (2016) http://dx.doi.org/10.1016/j.nano.2016.08.006 (in press).
[58] C.B. Hall, Respiratory syncytial virus in young children, Lancet 375 (2010) 1500–1502, http://dx.doi.org/10.1016/S0140-6736(10)60401-1.